

1 **Chondroitin sulfate proteoglycan Windpipe modulates Hedgehog signaling in *Drosophila***

2
3 ¹Masahiko Takemura, ²Fredrik Noborn, ²Jonas Nilsson, ¹Eriko Nakato, ¹Tsu-Yi Su, ²Göran Larson, and
4 ¹Hiroshi Nakato

5
6 1 Department of Genetics, Cell Biology, and Development, University of Minnesota, Minneapolis, MN,
7 USA

8 2 Department of Clinical Chemistry and Transfusion Medicine, Institute of Biomedicine, University of
9 Gothenburg, Gothenburg, Sweden

10
11
12 **Abstract**

13
14 Proteoglycans, a class of carbohydrate-modified proteins, often modulate growth factor signaling on the
15 cell surface. However, the molecular mechanism by which proteoglycans regulate signal transduction is
16 largely unknown. In this study, using a recently-developed glycoproteomic method, we found that
17 Windpipe (Wdp) is a novel chondroitin sulfate proteoglycan (CSPG) in *Drosophila*. Wdp is a single-pass
18 transmembrane protein with leucin-rich repeat (LRR) motifs and bears three CS sugar chain attachment
19 sites in the extracellular domain. Here we show that Wdp modulates the Hedgehog (Hh) pathway.
20 Overexpression of *wdp* inhibits Hh signaling in the wing disc, which is dependent on its CS chains and
21 the LRR motifs. Conversely, loss of *wdp* leads to the upregulation of Hh signaling. Furthermore,
22 knockdown of *wdp* increase the cell surface accumulation of Smoothened (Smo), suggesting that Wdp
23 inhibits Hh signaling by regulating Smo stability. Our study demonstrates a novel role of CSPG in
24 regulating Hh signaling.
25

26 Introduction

27
28 Spatial and temporal regulation of growth factor signaling pathways is essential to proper development
29 and disease prevention. Cell surface signaling events, such as ligand-receptor interactions, are often
30 modulated by proteoglycans (D. Xu & Esko, 2014). Proteoglycans are carbohydrate-modified proteins
31 that are found on the cell surface and in the extracellular matrix. They are composed of a core protein and
32 one or more glycosaminoglycans (GAGs) covalently attached to specific serine residues on the core
33 protein. GAGs are long, unbranched, and highly sulfated polysaccharide chains consisting of a repeating
34 disaccharide unit. Based on the composition of the disaccharide units, proteoglycans are classified into
35 several types, including heparan sulfate proteoglycans (HSPGs) and chondroitin sulfate proteoglycans
36 (CSPGs).

37
38 HSPGs function as co-receptors by interacting with a wide variety of ligands and modulate signaling
39 activities (Holt & Dickson, 2005; J.-S. Lee & Chien, 2004; Lindahl & Li, 2009; Poulain & Yost, 2015; D.
40 Xu & Esko, 2014). *Drosophila* offers a powerful model system to study the functions of HSPGs *in vivo*
41 because of its sophisticated molecular genetic tools and minimal genetic redundancy in genes encoding
42 core proteins and HS synthesizing/modifying enzymes (Lander & Selleck, 2000; Nakato & Li, 2016;
43 Perrimon & Bernfield, 2000; Takemura & Nakato, 2015). *In vivo* studies using the *Drosophila* model
44 have shown that HSPGs orchestrate information from multiple ligands in a complex extracellular milieu
45 and sculpt the signal response landscape in a tissue {Nakato & Li, 2016}. However, the molecular
46 mechanisms of co-receptor activities of HSPGs still remain a fundamental question. Our previous studies
47 predict that there are unidentified molecules involved in the molecular recognition events on the cell
48 surface (Akiyama et al., 2008).

49
50 In addition to HS, *Drosophila* produces CS, another type of GAG (Toyoda, Kinoshita-Toyoda, & Selleck,
51 2000). CSPGs are well known as major structural components of the extracellular matrix. CSPGs have
52 also been shown to modulate signaling pathways, including Hedgehog (Hh), Wnt, and fibroblast growth
53 factor signaling (Cortes, Baria, & Schwartz, 2009; Townley & Bülow, 2018). Given the structural
54 similarities between CS and HS, CSPGs may have modulatory, supportive and/or complementary
55 functions to HSPGs. However, the mechanisms by which CSPGs function as a co-receptor are unknown.
56 In contrast to a large number of studies on HSPGs, very few CSPGs have been identified and analyzed in
57 *Drosophila* (Momota, Naito, Ninomiya, & Ohtsuka, 2011). Unlike HSPGs, CSPG core proteins are not
58 well conserved between species (Olson, Bishop, Yates, Oegema, & Esko, 2006). Therefore, the
59 identification of CSPGs cannot rely on the sequence homology to mammalian counterparts.

60
61 Recently, we have developed a glycoproteomic method to identify novel proteoglycans (Noborn et al.,
62 2016; 2018; 2015). Briefly, this method includes trypsinization of protein samples, followed by
63 enrichment of glycopeptides using strong anion exchange (SAX) chromatography. After enzymatic
64 digestion of HS/CS chains, the glycopeptides bearing a linkage glycan structure common to HS and CS
65 chains are identified using nano-liquid chromatography-tandem mass spectrometry (nLC-MS/MS). This
66 method has successfully identified novel CSPGs in humans (Noborn et al., 2015) and *Caenorhabditis*
67 *elegans* (Noborn et al., 2018).

68
69 To study the function of CSPGs in signaling, we applied the glycoproteomic method to identify
70 previously unrecognized CSPGs in *Drosophila*. We found that Windpipe (Wdp) is a novel CSPG and
71 affects Hh signaling. Overexpression of *wdp* inhibits Hh signaling in the wing disc. This inhibitory effect
72 of Wdp on Hh signaling is dependent on its CS chains and LRR motifs. Consistent with the
73 overexpression analysis, loss of *wdp* increases Hh signaling. Loss of *wdp* also increases cell surface
74 accumulation of Smoothed (Smo), the Hh signaling transducer. Therefore, we propose that Wdp
75 downregulates Hh signaling by disrupting cell surface accumulation of Smo.

76

77 Results

78

79 A glycoproteomic approach identified Wdp as a novel *Drosophila* CSPG

80

81 We investigated the potential presence of CSPGs in *Drosophila* using our recently-developed
82 glycoproteomic approach that identifies core proteins and its CS attachment sites. A general workflow for
83 the sample preparation, CS-glycopeptide enrichment, LC-MS/MS analysis and the subsequent data
84 analysis is shown in Fig. 1A. Briefly, *Drosophila* third-instar larvae were collected from two different
85 genotypes (wild type [Oregon-R] and a loss-of-function mutant for *tout-velu* [*ttv*⁵²⁴]) and the material was
86 homogenized in ice-cold acetone. *ttv* encodes a *Drosophila* HS polymerase, and *ttv* mutants lack HS
87 chains (Toyoda et al., 2000). The samples were incubated with trypsin and then passed over an anion
88 exchange column equilibrated with a low-salt buffer. This procedure enriches for CS-attached
89 glycopeptides as the matrix retains anionic polysaccharides and their attached peptides, whereas neutral or
90 positively charged peptides flow through the column. The bound structures were eluted stepwise with
91 three buffers of increasing sodium chloride concentrations. The resulting fractions were treated with
92 chondroitinase ABC. This procedure reduces the lengths of the CS chains and generates a residual
93 hexasaccharide structure still attached to the core protein. The chondroitinase-treated fractions were
94 analyzed with positive mode nLC-MS/MS and an automated search strategy was used to identify CS
95 modified peptides in the generated data set (Noborn et al., 2015).

96

97 The analysis revealed the Windpipe (Wdp) protein as a novel CSPG, which was modified with three CS-
98 polysaccharides on two unique peptides (Fig. 1B and 1C). We detected Wdp glycopeptides from both
99 wild-type and *ttv* mutant samples, further supporting that Wdp bears CS chains, not HS. One of the
100 identified precursor ions (m/z 983.38; 3+) equated to the mass of a peptide with a
101 SDQVEGSGDLSETNMELK sequence, derived from the middle part of the protein (amino acids 276–
102 293) (Fig. 1B). The peptide was modified with one hexasaccharide structure and one methionine
103 oxidation. The measured mass (2947.1186 Da) deviated - 3.27 ppm from the theoretical value. The other
104 identified precursor ion (m/z 1276.76; 4+) equated to the mass of a peptide with a
105 EEHIVKDEDEDDEGSGSGGGLLIIPDPSK sequence, located in proximity to the previous peptide
106 (amino acids 320–348) (Fig. 1C). The peptide was found to be modified with two hexasaccharide
107 structures and where one of the hexasaccharides were modified with one phosphate modification. The
108 measured mass (5102.9389 Da) deviated +3.05 ppm from the theoretical value. Detailed inspection of the
109 spectra revealed several b- and y-ions as well as the prominent diagnostic oxonium ion at m/z 362.1,
110 corresponding to the disaccharide [GlcAGalNAc-H₂O+H]⁺ (Fig. 1B and 1C). Furthermore, one of the
111 glycans in Fig 1C was found modified with one phosphate group at a xylose residue (peptide + xylose +
112 phosphate, m/z 1625.70; 2+).

113

114 Wdp is a single-pass transmembrane protein containing four leucine rich repeat (LRR) motifs in the
115 extracellular domain (Huff, Kingsley, Miller, & Hoshizaki, 2002). The three CS attachment sites (S282,
116 S334, and S336) revealed by our glycoproteomic analysis are located in the extracellular domain (Fig.
117 3A). Interestingly, a recent study reported that Wdp negatively regulates JAK–STAT signaling by
118 promoting internalization and lysosomal degradation of the Domeless (Dome) receptor (W. Ren et al.,
119 2015). We further investigated the role of Wdp, a novel CSPG, in signal transduction.

120

121

122 Overexpression of *wdp* inhibits Hh signaling

123

124 The growth and patterning of the *Drosophila* wing are controlled by multiple signaling pathways,
125 including Decapentaplegic (Dpp; the *Drosophila* BMP), Wingless (Wg; the *Drosophila* Wnt), and
126 Hedgehog (Hh) signaling (Baena-Lopez, Nojima, & Vincent, 2012; Tabata & Takei, 2004). To determine
127 the role of *wdp* in these developmental signaling pathways, we first asked whether overexpression of *wdp*

128 affects adult wing morphology. When *wdp* was overexpressed in the wing pouch using *Bx^{MS1096}-GAL4*
129 (Capdevila & Guerrero, 1994) (*Bx^{MS1096}>wdp*), the wing size was reduced compared to that of control
130 flies (*Bx^{MS1096}>*) (Fig. 3C; compared to Fig. 3B). In addition, the distance between longitudinal wing veins
131 3 and 4 (L3 and L4) was aberrantly narrower. This decreased distance between L3 and L4 is indicative of
132 reduced Hh signaling during wing development (Mullor, Calleja, Capdevila, & Guerrero, 1997; Strigini &
133 Cohen, 1997).

134
135 Hh is produced in the posterior compartment of the wing disc and spreads towards the anterior
136 compartment where Hh signaling induces target genes expression in a concentration-dependent manner
137 (Briscoe & Thérond, 2013; Gradilla & Guerrero, 2013; Hartl & Scott, 2014). Expression of high-
138 threshold target genes, such as Patched (Ptc; the Hh receptor) (Capdevila, Pariente, Sampedro, Alonso, &
139 Guerrero, 1994) and Engrailed (En) (Patel et al., 1989) are induced in anterior cells near the
140 anteroposterior compartment boundary by high levels of Hh signaling (Jia, Tong, Wang, Luo, & Jiang,
141 2004) (Fig. 2A and 2E). Low levels of Hh signaling induce the expression of *dpp* and the accumulation of
142 full-length Cubitus interruptus (Ci; the transcriptional factor of Hh signaling) in a broader region (more
143 distant away from the anteroposterior boundary) (Fig. 2A and 2C). To determine if Hh signaling is indeed
144 affected by *wdp*, we overexpressed *wdp* in the dorsal compartment of the wing disc using *ap-GAL4*
145 (Calleja, Moreno, Pelaz, & Morata, 1996; O'Keefe, Thor, & Thomas, 1998). We found that *wdp*
146 overexpression in the dorsal compartment reduced the expression domains of both “high-threshold”
147 targets (Ptc and En) and “low-threshold” targets (*dpp-lacZ¹⁰⁶³⁸*, a reporter for *dpp* expression, and full-
148 length Ci) compared to those in the ventral compartment (Fig. 2B, 2D, and 2F). Notably, overexpression
149 of *wdp* did not affect the pattern of a *hh* transcriptional reporter *hh-lacZ^{P30}* (J. J. Lee, Kessler, Parks, &
150 Beachy, 1992) (Fig. 2F). Together, *wdp* acts as a negative regulator of Hh signaling without affecting *hh*
151 transcription

152
153 On the other hand, Wdp does not appear to affect Dpp and Wg pathways. When *wdp* is overexpressed
154 using *ap-GAL4* or *hh-GAL4* (a posterior compartment-specific GAL4 driver) (Tanimoto, Itoh, Dijke, &
155 Tabata, 2000), we did not observe apparent defects in Dpp signaling activity, which was monitored by the
156 expression of phosphorylated Mad (pMad) and Spalt major (Salm) (readouts of Dpp signaling). Similarly,
157 no changes in expression of Senseless (Sens) and Distal-less (Dll) (readouts of Wg signaling) were
158 detected (Fig. S1). These results are consistent with a previous report (W. Ren et al., 2015).

159
160 We also found that overexpression of *wdp* induces massive apoptosis, as detected with anti-cleaved
161 Caspase-3 antibody (Fig. S2B). This likely contributed to the smaller adult wing phenotype observed in
162 *Bx^{MS1096}>wdp* flies. It was recently reported that Hh signaling is required for cell survival in wing disc
163 cells (Lu, Wang, & Shen, 2017). To determine whether reduced Hh signaling is responsible for the
164 observed apoptosis, we first asked if reduced Hh signaling results in apoptosis. We inhibited Hh signaling
165 either by expressing an RNAi construct targeting *smo* (TRiP.HMC03577) (Fig. S2E), or by
166 overexpressing *ptc* in the dorsal compartment using *ap-GAL4*. We found that neither treatment caused
167 massive apoptosis (Fig. S2F and S2G), indicating that reduced Hh signaling is not sufficient to induce
168 massive apoptosis in the wing disc. Furthermore, coexpression of a constitutively active form of Smo
169 with Wdp did not suppress apoptosis in the wing disc (Fig. S2H). Thus, these results suggest that
170 overexpression of *wdp* induces apoptosis, independent of reduced Hh signaling.

171

172

173 **CS and LRR motifs are necessary for Wdp to inhibit Hh signaling**

174

175 Next, we asked whether the CS chains of Wdp are required for its function. In a CSPG core-protein, CS is
176 attached to specific serine residues in the consensus serine-glycine dipeptide surrounded by acidic amino
177 acids (Esko & Zhang, 1996). We generated a *UAS-wdp^{AGAG}* construct in which all three serine residues
178 (S282, S334, and S336) are substituted with alanine residues so that CS cannot be attached to the core

179 protein (Fig. 3A). The *UAS-wdp^{AGAG}* construct was inserted in the same genomic location (ZH-86Fb;
180 (Bischof, Maeda, Hediger, Karch, & Basler, 2007)) as *UAS-wdp* using the *phiC31* site-specific integration
181 system (Groth, Fish, Nusse, & Calos, 2004) in order to ensure the same expression level of the UAS
182 transgenes.

183
184 We found that *Bx^{MS1096}>wdp^{AGAG}* adult wings did not display the reduction in the distance between L3 and
185 L4 (Fig. 3B). Consistent with this, the expression of Ptc, En, Ci, and *dpp-lacZ* in the wing disc were not
186 affected by *wdp^{AGAG}* overexpression in the dorsal compartment of the wing disc (Fig. 3E–G). These
187 results indicate that CS chains are required for Wdp's activity to downregulate Hh signaling.

188
189 To determine whether the LRR motifs and/or the intracellular domain of Wdp are necessary for inhibiting
190 Hh signaling, we generated several Myc-tagged mutant constructs (Fig. S3) and examined their activities.
191 Consistent with the earlier result (Fig. 2B), expression of a Myc-tagged Wdp (Myc:Wdp) led to the
192 narrower Ptc expression domain (Fig. 3G). A mutant *wdp* construct lacking LRR motifs (Myc:Wdp^{ΔLRRs})
193 failed to inhibit Hh signaling (Fig. 3H). On the other hand, a truncated construct lacking the intracellular
194 domain (Myc:Wdp^{ΔICD}) retained the ability to inhibit Hh signaling (Fig. 3I). Thus, in addition to CS
195 chains, the LRR motifs of Wdp are required for inhibiting Hh signaling.

196
197

198 **Wdp expression in the wing disc**

199
200 To monitor Wdp expression, we generated transgenic flies (*wdp^{KI.HA}* and *wdp^{KI.OLLAS}*) expressing epitope-
201 tagged Wdp protein from its endogenous locus. We inserted a spaghetti monster GFP with 10 copies of
202 HA or OLLAS tags (Nern, Pfeiffer, & Rubin, 2015; Viswanathan et al., 2015) near the C-terminus of
203 Wdp (after Q652; Fig. 4A) using CRISPR–Cas9-mediated homology-directed repair (Gratz et al., 2014;
204 X. Ren et al., 2014). The Wdp:HA expression was detected in the eye disc, adult midgut, and tracheal
205 system (Fig. S3), consistent with previous reports (Huff et al., 2002; W. Ren et al., 2015).

206
207 In the wing disc, Wdp:HA is expressed in most of the wing disc cells with enrichment in the basal side, as
208 detected by anti-HA antibody (Fig. 4B and 4C). This result was confirmed by anti-OLLAS antibody
209 staining of the *wdp^{KI.OLLAS}* wing discs (Fig. S3A and S3B). In the wing disc epithelium, mitotic nuclei
210 apically translocate, but the cells maintain contact with the basal lamina via actin-rich basal projection
211 (Ragkousi & Gibson, 2014). Interestingly, Wdp:HA is strongly enriched in such basal projections (Fig.
212 4A and 4D). However, physiological significance of this localization of Wdp in the basal projections of
213 mitotic cells is unknown.

214
215

216 **Loss of *wdp* leads to higher levels of Hh signaling**

217
218 To determine whether loss of *wdp* affects Hh signaling activity, we examined the effect of *wdp* RNAi
219 knockdown in the wing disc. Expression of a *wdp^{RNAi}* construct (TRiP.HMC06302) using *ap-GAL4* in
220 *wdp^{KI.HA/+}* flies led to the loss of Wdp:HA staining specifically in the dorsal compartment (Fig. 4E),
221 validating the efficacy of RNAi-mediated knockdown of *wdp*. We then examined the effect of *wdp*
222 knockdown on Hh signaling using the Ptc expression level as a readout of the Hh signaling activity. In
223 control wing discs (*ap>FLP*), the signal intensity of Ptc staining in the dorsal compartment is comparable
224 to that in the ventral compartment (Fig. 5B). On the other hand, *wdp^{RNAi}* expression using *ap-GAL4*
225 increased the signal intensity of Ptc staining only in the dorsal compartment (Fig. 5A and 5C). In
226 addition, we observed that the *dpp-lacZ* expression domain was expanded anteriorly by *wdp* knockdown
227 (Fig. 5D). In the adult wing, knockdown of *wdp* slightly expanded the distance between wing vein L3 and
228 L4 near the distal tip (Fig. 5J, compared to Fig. 5I). Thus, *wdp* RNAi knockdown results in a moderate
229 increase in Hh signaling.

230
231
232
233
234
235
236
237
238
239
240
241
242
243
244
245
246
247
248
249
250
251

To confirm the *wdp* knockdown phenotypes, we generated a loss-of-function allele of *wdp* (*wdp*^{KO.ΔCDS}), in which most of the *wdp* coding sequence was removed using CRISPR–Cas9-mediated defined deletion (Gratz et al., 2013) (Fig. 5E–G). *wdp*^{KO.ΔCDS} homozygous mutant clones were induced in the wing pouch using the FLP–FRT system with *nubbin* (*nub*)-*GAL4 UAS-FLP* and their effect on Hh signaling was examined using anti-Ptc antibody. Consistent with the RNAi knockdown results, we observed a modest increase of Ptc expression in cells mutant for *wdp* (Fig. 5H). Taken together, we conclude that *wdp* negatively regulates Hh signaling in the *Drosophila* wing.

Wdp inhibits Smo cell surface accumulation

The seven-pass transmembrane protein Smo is a key transducer of Hh signaling. In the absence of Hh, Ptc inhibits the phosphorylation of Smo, which is internalized and degraded (Zhu, Zheng, Suyama, & Scott, 2003). In the presence of Hh, restriction of Ptc on Smo is relieved, allowing Smo to accumulate on the cell surface and activate Hh signaling. Although *smo* transcription is ubiquitous, Smo protein expression levels are high in the posterior compartment of the wing disc where Ptc is not expressed (Fig. 6A) (Denef, Neubüser, Perez, & Cohen, 2000). We found that knockdown of *wdp* increases the cell surface accumulation of Smo (Fig. 6B). This result suggests that Wdp downregulates Hh signaling either by disrupting Smo translocation to the cell membrane or the stability of Smo on the cell surface.

252 Discussion

253
254 The molecular mechanism by which HSPG co-receptors regulate growth factor signaling remains a
255 central question in cell biology. Dally, a *Drosophila* HSPG of the glypican type, potentiates Dpp
256 signaling by stabilizing the ligand-receptor complex on the cell surface (Akiyama et al., 2008), suggesting
257 that controlling the rate of receptor-mediated internalization of the signaling complex is the basis for co-
258 receptor activity. However, it is still unknown how HSPGs affect endocytosis and internalization. Since
259 glypicans do not have an intracellular domain, it is likely that these molecules cooperate with other
260 factors (e.g. membrane proteins) to exert co-receptor activity. Thus, it is clear that there are many more
261 unknown factors involved in molecular recognition events on the cell surface. To understand the
262 molecular basis for cell communications, it is critical to identify novel cell surface players.

263
264 We found that in the wing disc, Wdp negatively regulates Hh signaling in a CS- and LRR motif-
265 dependent manner. It has also been reported that Wdp negatively regulates JAK–STAT signaling and
266 controls adult midgut homeostasis and regeneration (W. Ren et al., 2015). The authors showed that Wdp
267 interacts with the Dome receptor and promotes its endocytosis and lysosomal degradation. Thus, it is
268 interesting to test if Wdp interacts with Dome via CS chains to modulate JAK–STAT signaling. We
269 observed that Wdp affects cell surface accumulation of Smo, suggesting its role in regulating the stability
270 of Smo protein. Thus, it is possible that Wdp modulates these pathways via a similar mechanism:
271 controlling the internalization of Dome and Smo on the cell membrane.

272
273 It is worth noting that both JAK–STAT and Hh signaling, the two pathways negatively controlled by
274 Wdp, are also regulated by HSPGs. Dally-like, a glypican family of HSPGs, positively regulates Hh
275 signaling by interacting with Hh and Ptc (Desbordes & Sanson, 2003; M.-S. Kim, Saunders, Hamaoka,
276 Beachy, & Leahy, 2011; Lum, Yao, et al., 2003a; Williams et al., 2010; Yan et al., 2010). In the
277 developing ovary, Dally upregulates the JAK–STAT pathway (Y. Hayashi et al., 2012). Given the
278 importance of precise dosage control of oncogenic pathways, such as JAK–STAT and Hh signaling, this
279 dual proteoglycan system could play an important role in fine-tuning of the signaling output in order to
280 prevent cancer formation. In vertebrates, HSPGs and CSPGs show opposing effects in neural systems.
281 For example, axon growth is typically promoted by HSPGs but inhibited by CSPGs (Bandtlow &
282 Zimmermann, 2000; Coles et al., 2011; Kantor et al., 2004; Matsumoto, Irie, Inatani, Tessier-Lavigne, &
283 Yamaguchi, 2007; Silver & Miller, 2004; Van Vactor, Wall, & Johnson, 2006). Our findings suggest that
284 such competing effects of HSPGs and CSPGs may be a general mechanism for the precise control of
285 signaling cascades and pattern formation.

286
287 In addition to the functions in signaling, Wdp may play other roles. We found that overexpression of *wdp*
288 results in massive apoptosis in the wing disc, independent of Hh signaling inhibition (Fig. S2). Since
289 CSPGs are well known for structural functions, an excess amount of Wdp may affect the epithelial
290 integrity of the wing disc, leading to subsequent apoptosis. Our observation that Wdp is enriched on the
291 basal side of the wing disc and adult midgut cells (Fig. 4B and S3F) suggests that Wdp may interact with
292 components of the basement membrane, which surrounds these organs.

293
294 In mice, sulfated CS is necessary for Indian hedgehog (Ihh) signaling in the developing growth plate
295 (Cortes et al., 2009). Ihh and Sonic hedgehog (Shh) bind to CS (Cortes et al., 2009; Whalen, Malinauskas,
296 Gilbert, & Siebold, 2013; F. Zhang, McLellan, Ayala, Leahy, & Linhardt, 2007). Thus, it will be
297 interesting to check if Wdp interacts with Hh via its CS chains.

298
299 Previous studies also reported that *wdp* is associated with aggressive behaviors in *Drosophila* species.
300 *wdp* is upregulated in the head of socially isolated male flies, which exhibit more aggressive behaviors
301 than males raised in groups (L. Wang, Dankert, Perona, & Anderson, 2008). Also, *wdp* expression is
302 slightly higher in the brain of *Drosophila prolongata*, which is more aggressive compared to its closely-

303 related species (Kudo et al., 2017). Since CSPGs are important in neuronal patterning (Saied-Santiago &
304 Bülow, 2018), it is interesting to study the molecular mechanisms behind Wdp's effect on *Drosophila*
305 behavior.

306

307 In mammals, there are a class of CSPG molecules with LRR motifs (small leucine-rich proteoglycans, or
308 SLRPs). A number of SLRP members are known as causative genes of human genetic disorders (Bech-
309 Hansen et al., 2000; Pusch et al., 2000; Schaefer & Iozzo, 2008). Although Wdp does not have cysteine-
310 rich regions that are commonly found in mammalian SLRPs, MARRVEL (ver 1.1) (J. Wang et al., 2017)
311 reports that *wdp* is a potential *Drosophila* ortholog of the human *NYX* gene (nyctalopin), a member of
312 SLRPs (DIPOT score 1 (Hu et al., 2011)). Mutations in *NYX* cause X-linked congenital stationary night
313 blindness (Bech-Hansen et al., 2000; Pusch et al., 2000). Further studies on Wdp will provide a novel
314 insight into the function of these disease-related human counterparts.

315

316

317 **Materials and Methods**

318

319 **Preparation of glycosaminoglycan-glycopeptides and LC-MS/MS analysis**

320

321 Glycosaminoglycan-glycopeptide samples were prepared from wild-type (Oregon-R) and *ttv* mutant
322 (*ttv*⁵²⁴) third-instar larvae as previously described (Noborn et al., 2015; 2018). Briefly, 200-400 third
323 instar larvae (wet weight; 200-400 mg) were lyophilized and homogenized using a motor pestle in 1 ml of
324 ice-cold acetone. After extensive washes with acetone, the insoluble fraction was recovered by
325 centrifugation. After overnight desiccation, the pellet was dissolved in 1.5 ml 1% CHAPS lysis buffer and
326 boiled for 10 min at 96°C. The sample was adjusted to 2 mM MgCl₂ and incubated with 3 μl Benzonase
327 (MilliporeSigma, Burlington, MA) at 37°C for three hours. After heat-inactivation of Benzonase, the
328 sample was centrifuged and the supernatant was collected in a new tube.

329

330 An aliquot of the preparation (1 mg of protein) was further used. The sample was reduced and alkylated
331 in 1 ml 50 mM NH₄HCO₃, and trypsinized at 37°C overnight with 20 μg trypsin (Promega, Madison, WI).
332 The digested samples were applied onto DEAE (GE Healthcare, Chicago, IL) columns (600 μl) at 4°C.
333 The columns were washed with three different low-salt washing solutions at 4°C: 50 mM Tris-HCl, 100
334 mM NaCl, pH 8.0; 50 mM NaAc, 100 mM NaCl, pH 4.0; and 100 mM NaCl. The glycopeptides that
335 were bound to DEAE were eluted stepwise with three buffers with increasing sodium chloride
336 concentrations at 4°C: 4 ml 250 mM NaCl, 400 mM NaCl, 800 mM NaCl, and 3 ml 1500 mM NaCl.
337 Each fraction was desalted using PD10-columns (GE Healthcare).

338

339 All fractions were lyophilized and the salt-free samples were then individually treated with 1 mU of
340 chondroitinase ABC (Sigma-Aldrich, St. Louis, MO) for 3 h at 37°C. Prior to MS-analysis, the samples
341 were desalted using a C18 spin column (8 mg resin) according to the manufacturer's protocol (Thermo
342 Fisher Scientific, Waltham, MA). LC-MS/MS analysis was performed as previously described (Noborn et
343 al., 2015; 2018). In brief, the samples were analyzed on a Q Exactive mass spectrometer coupled to an
344 Easy-nLC 1000 system (Thermo Fisher Scientific). Briefly, glycopeptides (2-μl injection volume) were
345 separated using an analytical column with Reprosil-Pur C18-AQ particles (Dr. Maisch GmbH,
346 Ammerbuch, Germany). The following gradient was run at 300 nl/min; from 7-35 % B-solvent
347 (acetonitrile in 0.2% formic acid) over 75 min, to 100 % B-solvent over 5 min, with a final hold at 100%
348 B-solvent for 10 min. The A-solvent was 0.2% formic acid. Spectra were recorded in positive ion mode
349 and MS scans were performed at 70,000 resolution with a mass range of *m/z* 600–1800. The MS/MS
350 analysis was performed in a data-dependent mode, with the top ten most abundant charged precursor ions
351 in each MS scan selected for fragmentation (MS2) by higher energy collision dissociation with
352 normalized collision energy values of 30. The MS2 scans were performed at a resolution of 35,000 (at *m/z*
353 200). The data analyses were performed as previously described (Noborn et al., 2015) with some small
354 adjustments. In brief, the HCD.raw spectra were converted to Mascot .mgf format using Mascot distiller
355 (version 2.3.2.0, Matrix Science, London, UK). The ions were presented as singly protonated in the
356 output Mascot file. Searches were performed using an in-house Mascot server (version 2.3.02) with the
357 enzyme specificity set to *Trypsin*, and then to *Semitypsin*, allowing for one or two missed cleavages, in
358 subsequent searches on *Drosophila* sequences of the UniprotKB (42, 507, sequences, 2018-06-18). The
359 peptide tolerance was set to 10 parts per million (ppm) and fragment tolerance was set to 0.01 Da. The
360 searches were allowed to include variable modifications at serine residues of the residual hexasaccharide
361 structure [GlcA(-H₂O)GalNAcGlcAGalGalXyl-O-] with 0 (C₃₇H₅₅NO₃₀, 993.2809 Da), 1 (C₃₇H₅₅NO₃₃S,
362 1073.2377 Da), or 2 (C₃₇H₅₅NO₃₆S₂, 1153.1945 Da) sulfate groups attached.

363

364

365 **Fly husbandry and fly strains, and transgenic flies**

366

367 The following fly strains were used in this study:

368
369 Oregon-R, *w¹¹¹⁸* (Bloomington Drosophila Stock Center [BDSC] #5905), *ttv⁵²⁴* (Takei, 2004), *ap-GAL4*
370 (O'Keefe et al., 1998), *hh-GAL4* (Tanimoto et al., 2000), *Bx^{MS1096}-GAL4* (BDSC #8860) (Capdevila &
371 Guerrero, 1994), *ABI-GAL4* (BDSC #1824) (Tavsanli et al., 2004), *elav^{C155}>mCD8:GFP* (BDSC #5146)
372 (Lin & Goodman, 1994), *UAS-GFP* (BDSC #1521), *UAS-tdTomato* (BDSC #36327 and #36328), *UAS-*
373 *FLP* (BDSC #4539 and #4540), *UAS-ptc* (BDSC #44614), *nub-GAL4* (BDSC #25754), *FRT42D 2xUbi-*
374 *GFP*, *UAS-smo:GFP* (BDSC #44624), *UAS-FLAG:smo^{Act}* (BDSC #44621), *UAS-wdp^{RNAi}*
375 (TRiP.HMC06302, BDSC #66004), *UAS-wdp^{RNAi}* (TRiP.HM05118, BDSC #28907), *UAS-smo^{RNAi}*
376 (TRiP.HMC03577, BDSC #53348), *hh-lacZ^{P30}* (a gift from Gary Struhl) (J. J. Lee et al., 1992), *dpp-*
377 *lacZ¹⁰⁶³⁸* (BDSC #12379) (Zecca, Basler, & Struhl, 1995), *vas-Cas9* (BDSC #55821), *esg-GAL4* (DGRC
378 #113886) (S. Hayashi et al., 2002). The *UAS-wdp*, *UAS-wdp^{AGAG}*, *UAS-Myc:wdp*, *UAS-Myc:wdp^{ALRRs}*,
379 *UAS-Myc:wdp^{AI}*, *wdp^{KO.ACDS}*, *wdp^{KI.HA}*, *wdp^{KI.OLLAS}* flies were generated in this study. A full list of
380 genotypes used in this study can be found in Table S1.

381
382 For constructing *UAS-wdp*, *wdp* CDS (corresponding to wdp-RA-E in FlyBase) was inserted into the
383 XhoI- and XbaI-digested pJFRC7 vector (a gift from Gerald Rubin; Addgene # 26220) (Pfeiffer et al.,
384 2010) using NEBuilder HiFi DNA Assembly Master Mix (New England Biolabs [NEB], Ipswich, MA,
385 E2621S). Similarly, *wdp^{AGAG}* (S282A, S334A, and S336A), *Myc:wdp*, *Myc:wdp^{ALRRs}*, and *Myc:wdp^{AI}*
386 were inserted into the pJFRC7 vector. The UAS transgenic flies were generated using *phiC31* integrase-
387 mediated transgenesis at the ZH-86Fb attP (FBti0076525) integration site. Embryonic injection was
388 performed by BestGene Inc (Chino Hills, CA). Primers used in this study will be available upon request.

389
390 To generate the *wdp^{KO.ACDS}* allele, two sgRNAs (pU6-sgRNA-wdp-1 and pU6-sgRNA-wdp-2) were
391 introduced to delete the *wdp* CDS. To construct sgRNA plasmids, 5' -
392 CTTCGACAGGGCCAACCAGGCGGTC - 3' and 5' - AAACGACCGCCTGGTTGGCCCTGTC - 3'
393 were annealed (pU6-sgRNA-wdp-1); and 5' - CTTCGAGTGGCCATTGATCACCTGG - 3' and 5' -
394 AAACCCAGGTGATCAATGGCCACTC - 3' (pU6-sgRNA-wdp-2) were annealed and ligated in the
395 BbsI-digested pU6-BbsI-chiRNA plasmid (a gift from Melissa Harrison, Kate O'Connor-Giles, and Jill
396 Wildonger; Addgene #45946) (Gratz et al., 2013). A mixture of 50 ng/μl of pU6-sgRNA-wdp-1 and pU6-
397 sgRNA-wdp-2 was injected into the embryos of the *vas-Cas9* flies, which express Cas9 under the control
398 of the germline *vasa* regulatory elements (Gratz et al., 2014), by BestGene Inc. The *wdp^{KO.ACDS}* allele was
399 screened by PCR and verified by Sanger sequencing.

400
401 To generate the *wdp^{KI.HA}* allele, we constructed a donor plasmid, which contained a Gly-Gly-Ser linker,
402 smGFP-HA, and approximately 1-kb homology arms to *wdp* flanking the linker and smGFP-HA, for
403 homology-directed repair. smGFP-HA and the *wdp* homology sequences on either side of the targeted
404 DSB were PCR-amplified from pJFRC201-10XUAS-FRT>STOP>FRT-myr:smGFP-HA (a gift from
405 Gerald Rubin; Addgene plasmid #63166) (Nern et al., 2015) and genomic DNA extracted from the *vas-*
406 *Cas9* flies, respectively. These fragments were cloned into the pHD-DsRed-attP backbone (a gift from
407 Melissa Harrison, Kate O'Connor-Giles and Jill Wildonger; Addgene #51019) (Gratz et al., 2014) using
408 NEBuilder HiFi DNA Assembly Master Mix (NEB, E2621S). Similarly, we generated a donor plasmid
409 with OLLAS tags amplified from pJFRC210-10XUAS-FRT>STOP>FRT-myr:smGFP-OLLAS (a gift
410 from Gerald Rubin; Addgene plasmid #63170) (Nern et al., 2015). A mixture of 50 ng/μl of pU6-sgRNA-
411 wdp-2 and 125 ng/μl of each donor plasmid was injected into the *vas-Cas9* embryos by BestGene Inc.
412 The *wdp^{KI.HA}* and *wdp^{KI.OLLAS}* alleles were screened by PCR and verified by Sanger sequencing.

413
414 Flies were raised on a standard cornmeal fly medium at 25°C unless otherwise indicated.

415
416
417 **Mosaic analysis**

418

419 The *wdp*^{KO. ΔCDS} homozygous clones were generated by FLP/FRT-mediated mitotic recombination (T. Xu
420 & Rubin, 1993). The FLP expression was induced by *nub-GAL4 UAS-FLP*.

421
422

423 **Immunohistochemistry**

424

425 Third-instar larval imaginal discs were stained as described previously (Takemura & Adachi-Yamada,
426 2011) with some modifications. Wing discs were dissected from third-instar wandering larvae in
427 phosphate-buffered saline (PBS, pH 7.4) and subsequently fixed in 3.7% formaldehyde in PBS for 15 min
428 at room temperature. After three 10-min washes with PBST (PBS containing 0.1% (vol/vol) Triton X-100
429 [Sigma, T8532]), the samples were incubated in primary antibodies overnight at 4°C. After three 10-min
430 washes with PBST, the samples were incubated with Alexa Fluor-conjugated secondary antibodies
431 (1:500, Thermo Fisher Scientific) overnight at 4°C or 2 hours at room temperature. After three 10-min
432 washes with PBST, the samples were stained with 1 μg/ml DAPI (Thermo Fisher Scientific, 62248) and
433 subsequently mounted in VECTASHIELD Antifade Mounting Medium (Vector Laboratories,
434 Burlingame, CA, H-1000). F-actin was stained with Alexa Fluor 568 phalloidin (Thermo Fisher
435 Scientific, A12380). Adult midguts were dissected and immunostained as previously described
436 (Takemura & Nakato, 2017). Images were acquired on a LSM710 confocal microscope (Carl Zeiss,
437 Oberkochen, Germany). For quantification of Ptc staining, images were acquired with the same condition,
438 and fluorescence intensity was measured in a set area with Fiji (Schindelin et al., 2012).

439

440

441 **Antibodies**

442

443 The primary antibodies used were as follows: mouse anti-Ptc Apa 1 (1:20, Developmental Studies
444 Hybridoma Bank [DSHB], Iowa City, IA, deposited by Isabel Guerrero) (Capdevila et al., 1994), rat anti-
445 Ci 2A1 (1:20, DSHB, deposited by Robert Holmgren) (Motzny & Holmgren, 1995), chicken anti-β-
446 Galactosidase (1:2000, Abcam), mouse anti-En 4D9 (1:20, DSHB, deposited by Corey Goodman)
447 (Riggleman, Schedl, & Wieschaus, 1990), rabbit anti-pH3 (1:1000, Millipore, 06-570), rat anti-HA 3F10
448 (1:200, Roche, 11867423001), rabbit anti-HA C29F4 (1:1000, Cell Signaling, 3724), mouse anti-Smo
449 20C6 (1:50, DSHB, deposited by Philip Beachy) (Lum, Zhang, et al., 2003b), rabbit anti-pSmad3
450 (1:1000, Epitomics, 1880-1) (Smith, Machamer, Kim, Hays, & Marques, 2012), rabbit anti-Salm (1:30, a
451 gift from Scott Selleck), mouse anti-Dll 1:500 (1:500, a gift from Dianne Duncan) (D. M. Duncan,
452 Burgess, & Duncan, 1998), guinea pig anti-Sens (1:1000, a gift from Hugo Bellen) (Nolo, Abbott, &
453 Bellen, 2000), rabbit anti-cleaved Caspase-3 (1:200, Cell Signaling, 9661), rat anti-OLLAS L2 (1:500,
454 Novus Biologicals, NBP1-06713), mouse anti-Arm N2 7A1 (1:50, DSHB, deposited by Eric Wieschaus)
455 (Riggleman et al., 1990), mouse anti-Pros MR1A (1:50, DSHB, deposited by C.Q. Doe) (Campbell et al.,
456 1994), and mouse anti-Fas3 7G10 (1:50, DSHB, deposited by Corey Goodman) (Patel, Snow, &
457 Goodman, 1987). Alexa488, Alexa548, Alexa564 and Alexa633-conjugated secondary antibodies
458 (Thermo Fisher Scientific) were used at a dilution of 1:500.

459

460

461 **Adult wing preparation**

462

463 The left wings from female flies were dissected and mounted on slides using Canada balsam (Benz
464 Microscope, BB0020) as previously described (Takemura & Adachi-Yamada, 2011). Images were taken
465 using a ZEISS Stemi SV 11 microscope equipped with a Jenoptik ProgRes C3 digital camera.

466

467 **Acknowledgements**

468

469 We thank Melissa Harrison, Kate O'Connor-Giles, Jill Wildonger, Gary Struhl, Scott Selleck, Hugo
470 Bellen, the Bloomington Drosophila Stock Center (NIH P40OD018537), the Transgenic RNAi Project at
471 Harvard Medical School [NIH/NIGMS R01-GM08947], and the Drosophila Genomics Resource Center
472 (NIH 2P40OD010949) for sharing fly strains and plasmids. We also thank the Proteomics Core Facility at
473 the Sahlgrenska Academy, University of Gothenburg, Sweden for running all the MS analyses. This work
474 was supported by the National Institutes of Health (R01 GM115099) to H.N. M.T. held postdoctoral
475 fellowships from the Japan Society for the Promotion of Science and the Uehara Memorial Foundation.

476

477

478 **Competing interests**

479

480 The authors declare no competing or financial interests.

481

482 **References**

- 483
- 484 Akiyama, T., Kamimura, K., Firkus, C., Takeo, S., Shimmi, O., & Nakato, H. (2008). Dally regulates
485 Dpp morphogen gradient formation by stabilizing Dpp on the cell surface. *Developmental Biology*,
486 *313*(1), 408–419. <http://doi.org/10.1016/j.ydbio.2007.10.035>
- 487 Baena-Lopez, L. A., Nojima, H., & Vincent, J.-P. (2012). Integration of morphogen signalling within the
488 growth regulatory network. *Current Opinion in Cell Biology*, *24*(2), 166–172.
489 <http://doi.org/10.1016/j.ceb.2011.12.010>
- 490 Bandtlow, C. E., & Zimmermann, D. R. (2000). Proteoglycans in the developing brain: new conceptual
491 insights for old proteins. *Physiological Reviews*, *80*(4), 1267–1290.
492 <http://doi.org/10.1152/physrev.2000.80.4.1267>
- 493 Bech-Hansen, N. T., Naylor, M. J., Maybaum, T. A., Sparkes, R. L., Koop, B., Birch, D. G., et al. (2000).
494 Mutations in NYX, encoding the leucine-rich proteoglycan nyctalopin, cause X-linked complete
495 congenital stationary night blindness. *Nature Genetics*, *26*(3), 319–323. <http://doi.org/10.1038/81619>
- 496 Bischof, J., Maeda, R. K., Hediger, M., Karch, F., & Basler, K. (2007). An optimized transgenesis system
497 for Drosophila using germ-line-specific phiC31 integrases. *Proceedings of the National Academy of*
498 *Sciences of the United States of America*, *104*(9), 3312–3317.
499 <http://doi.org/10.1073/pnas.0611511104>
- 500 Briscoe, J., & Théron, P. P. (2013). The mechanisms of Hedgehog signalling and its roles in
501 development and disease. *Nature Reviews. Molecular Cell Biology*, *14*(7), 416–429.
502 <http://doi.org/10.1038/nrm3598>
- 503 Calleja, M., Moreno, E., Pelaz, S., & Morata, G. (1996). Visualization of gene expression in living adult
504 Drosophila. *Science (New York, NY)*, *274*(5285), 252–255.
- 505 Campbell, G., Göring, H., Lin, T., Spana, E., Andersson, S., Doe, C. Q., & Tomlinson, A. (1994). RK2, a
506 glial-specific homeodomain protein required for embryonic nerve cord condensation and viability in
507 Drosophila. *Development (Cambridge, England)*, *120*(10), 2957–2966.
- 508 Capdevila, J., & Guerrero, I. (1994). Targeted expression of the signaling molecule decapentaplegic
509 induces pattern duplications and growth alterations in Drosophila wings. *The EMBO Journal*, *13*(19),
510 4459–4468.
- 511 Capdevila, J., Pariente, F., Sampedro, J., Alonso, J. L., & Guerrero, I. (1994). Subcellular localization of
512 the segment polarity protein patched suggests an interaction with the wingless reception complex in
513 Drosophila embryos. *Development (Cambridge, England)*, *120*(4), 987–998.
- 514 Coles, C. H., Shen, Y., Tenney, A. P., Siebold, C., Sutton, G. C., Lu, W., et al. (2011). Proteoglycan-
515 specific molecular switch for RPTP σ clustering and neuronal extension. *Science (New York, NY)*,
516 *332*(6028), 484–488. <http://doi.org/10.1126/science.1200840>
- 517 Cortes, M., Baria, A. T., & Schwartz, N. B. (2009). Sulfation of chondroitin sulfate proteoglycans is
518 necessary for proper Indian hedgehog signaling in the developing growth plate. *Development*
519 *(Cambridge, England)*, *136*(10), 1697–1706. <http://doi.org/10.1242/dev.030742>
- 520 Denef, N., Neubüser, D., Perez, L., & Cohen, S. M. (2000). Hedgehog induces opposite changes in
521 turnover and subcellular localization of patched and smoothened. *Cell*, *102*(4), 521–531.
- 522 Desbordes, S. C., & Sanson, B. (2003). The glypican Dally-like is required for Hedgehog signalling in the
523 embryonic epidermis of Drosophila. *Development (Cambridge, England)*, *130*(25), 6245–6255.
524 <http://doi.org/10.1242/dev.00874>
- 525 Duncan, D. M., Burgess, E. A., & Duncan, I. (1998). Control of distal antennal identity and tarsal
526 development in Drosophila by spineless-aristopedia, a homolog of the mammalian dioxin receptor.
527 *Genes & Development*, *12*(9), 1290–1303.
- 528 Esko, J. D., & Zhang, L. (1996). Influence of core protein sequence on glycosaminoglycan assembly.
529 *Current Opinion in Structural Biology*, *6*(5), 663–670.
- 530 Gradilla, A.-C., & Guerrero, I. (2013). Hedgehog on the move: a precise spatial control of Hedgehog
531 dispersion shapes the gradient. *Current Opinion in Genetics & Development*, *23*(4), 363–373.
532 <http://doi.org/10.1016/j.gde.2013.04.011>

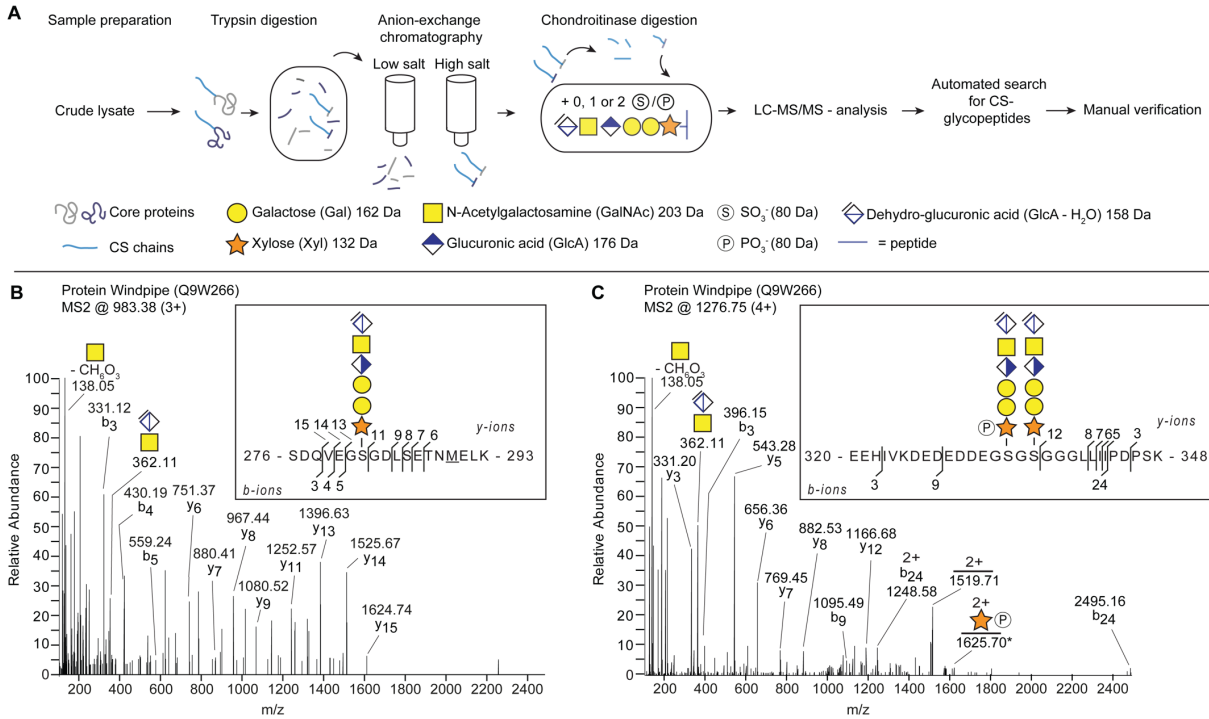
- 533 Gratz, S. J., Cummings, A. M., Nguyen, J. N., Hamm, D. C., Donohue, L. K., Harrison, M. M., et al.
534 (2013). Genome engineering of *Drosophila* with the CRISPR RNA-guided Cas9 nuclease. *Genetics*,
535 *194*(4), 1029–1035. <http://doi.org/10.1534/genetics.113.152710>
- 536 Gratz, S. J., Ukken, F. P., Rubinstein, C. D., Thiede, G., Donohue, L. K., Cummings, A. M., & O'Connor-
537 Giles, K. M. (2014). Highly specific and efficient CRISPR/Cas9-catalyzed homology-directed repair
538 in *Drosophila*. *Genetics*, *196*(4), 961–971. <http://doi.org/10.1534/genetics.113.160713>
- 539 Groth, A. C., Fish, M., Nusse, R., & Calos, M. P. (2004). Construction of transgenic *Drosophila* by using
540 the site-specific integrase from phage phiC31. *Genetics*, *166*(4), 1775–1782.
- 541 Hartl, T. A., & Scott, M. P. (2014). Wing tips: The wing disc as a platform for studying Hedgehog
542 signaling. *Methods*, *68*(1), 199–206. <http://doi.org/10.1016/j.ymeth.2014.02.002>
- 543 Hayashi, S., Ito, K., Sado, Y., Taniguchi, M., Akimoto, A., Takeuchi, H., et al. (2002). GETDB, a
544 database compiling expression patterns and molecular locations of a collection of Gal4 enhancer
545 traps. *Genesis (New York, NY : 2000)*, *34*(1-2), 58–61. <http://doi.org/10.1002/gene.10137>
- 546 Hayashi, Y., Sexton, T. R., Dejima, K., Perry, D. W., Takemura, M., Kobayashi, S., et al. (2012).
547 Glypicans regulate JAK/STAT signaling and distribution of the Unpaired morphogen. *Development*
548 (*Cambridge, England*), *139*(22), 4162–4171. <http://doi.org/10.1242/dev.078055>
- 549 Holt, C. E., & Dickson, B. J. (2005). Sugar Codes for Axons? *Neuron*, *46*(2), 169–172.
550 <http://doi.org/10.1016/j.neuron.2005.03.021>
- 551 Hu, Y., Flockhart, I., Vinayagam, A., Bergwitz, C., Berger, B., Perrimon, N., & Mohr, S. E. (2011). An
552 integrative approach to ortholog prediction for disease-focused and other functional studies. *BMC*
553 *Bioinformatics*, *12*(1), 357. <http://doi.org/10.1186/1471-2105-12-357>
- 554 Huff, J. L., Kingsley, K. L., Miller, J. M., & Hoshizaki, D. K. (2002). *Drosophila* windpipe codes for a
555 leucine-rich repeat protein expressed in the developing trachea. *Mechanisms of Development*, *111*(1-
556 2), 173–176.
- 557 Jia, J., Tong, C., Wang, B., Luo, L., & Jiang, J. (2004). Hedgehog signalling activity of Smoothened
558 requires phosphorylation by protein kinase A and casein kinase I. *Nature*, *432*(7020), 1045–1050.
559 <http://doi.org/10.1038/nature03179>
- 560 Kantor, D. B., Chivatakarn, O., Peer, K. L., Oster, S. F., Inatani, M., Hansen, M. J., et al. (2004).
561 Semaphorin 5A is a bifunctional axon guidance cue regulated by heparan and chondroitin sulfate
562 proteoglycans. *Neuron*, *44*(6), 961–975. <http://doi.org/10.1016/j.neuron.2004.12.002>
- 563 Kim, M.-S., Saunders, A. M., Hamaoka, B. Y., Beachy, P. A., & Leahy, D. J. (2011). Structure of the
564 protein core of the glypican Dally-like and localization of a region important for hedgehog signaling.
565 *Proceedings of the National Academy of Sciences of the United States of America*, *108*(32), 13112–
566 13117. <http://doi.org/10.1073/pnas.1109877108>
- 567 Kudo, A., Shigenobu, S., Kadota, K., Nozawa, M., Shibata, T. F., Ishikawa, Y., & Matsuo, T. (2017).
568 Comparative analysis of the brain transcriptome in a hyper-aggressive fruit fly, *Drosophila*
569 *prolongata*. *Insect Biochemistry and Molecular Biology*, *82*, 11–20.
570 <http://doi.org/10.1016/j.ibmb.2017.01.006>
- 571 Lander, A. D., & Selleck, S. B. (2000). The elusive functions of proteoglycans: in vivo veritas. *The*
572 *Journal of Cell Biology*, *148*(2), 227–232.
- 573 Lee, J. J., Kessler, von, D. P., Parks, S., & Beachy, P. A. (1992). Secretion and localized transcription
574 suggest a role in positional signaling for products of the segmentation gene hedgehog. *Cell*, *71*(1),
575 33–50.
- 576 Lee, J.-S., & Chien, C.-B. (2004). When sugars guide axons: insights from heparan sulphate proteoglycan
577 mutants. *Nature Reviews Genetics*, *5*(12), 923–935. <http://doi.org/10.1038/nrg1490>
- 578 Lin, D. M., & Goodman, C. S. (1994). Ectopic and increased expression of Fasciclin II alters motoneuron
579 growth cone guidance. *Neuron*, *13*(3), 507–523.
- 580 Lindahl, U., & Li, J.-P. (2009). Interactions between heparan sulfate and proteins—design and functional
581 implications. *International Review of Cell and Molecular Biology*, *276*, 105–159.
582 [http://doi.org/10.1016/S1937-6448\(09\)76003-4](http://doi.org/10.1016/S1937-6448(09)76003-4)

- 583 Lu, J., Wang, D., & Shen, J. (2017). Hedgehog signalling is required for cell survival in Drosophila wing
584 pouch cells. *Scientific Reports*, 7(1), 11317. <http://doi.org/10.1038/s41598-017-10550-4>
- 585 Lum, L., Yao, S., Mozer, B., Rovescalli, A., Kessler, Von, D., Nirenberg, M., & Beachy, P. A. (2003a).
586 Identification of Hedgehog pathway components by RNAi in Drosophila cultured cells. *Science (New*
587 *York, NY)*, 299(5615), 2039–2045. <http://doi.org/10.1126/science.1081403>
- 588 Lum, L., Zhang, C., Oh, S., Mann, R. K., Kessler, von, D. P., Taipale, J., et al. (2003b). Hedgehog signal
589 transduction via Smoothed association with a cytoplasmic complex scaffolded by the atypical
590 kinesin, Costal-2. *Molecular Cell*, 12(5), 1261–1274.
- 591 Matsumoto, Y., Irie, F., Inatani, M., Tessier-Lavigne, M., & Yamaguchi, Y. (2007). Netrin-1/DCC
592 signaling in commissural axon guidance requires cell-autonomous expression of heparan sulfate. *The*
593 *Journal of Neuroscience : the Official Journal of the Society for Neuroscience*, 27(16), 4342–4350.
594 <http://doi.org/10.1523/JNEUROSCI.0700-07.2007>
- 595 Momota, R., Naito, I., Ninomiya, Y., & Ohtsuka, A. (2011). Drosophila type XV/XVIII collagen, Mp, is
596 involved in Wingless distribution. *Matrix Biology : Journal of the International Society for Matrix*
597 *Biology*, 30(4), 258–266. <http://doi.org/10.1016/j.matbio.2011.03.008>
- 598 Motzny, C. K., & Holmgren, R. (1995). The Drosophila cubitus interruptus protein and its role in the
599 wingless and hedgehog signal transduction pathways. *Mechanisms of Development*, 52(1), 137–150.
- 600 Mullor, J. L., Calleja, M., Capdevila, J., & Guerrero, I. (1997). Hedgehog activity, independent of
601 decapentaplegic, participates in wing disc patterning. *Development (Cambridge, England)*, 124(6),
602 1227–1237.
- 603 Nakato, H., & Li, J.-P. (2016). Functions of Heparan Sulfate Proteoglycans in Development: Insights
604 From Drosophila Models. *International Review of Cell and Molecular Biology*, 325, 275–293.
605 <http://doi.org/10.1016/bs.ircmb.2016.02.008>
- 606 Nern, A., Pfeiffer, B. D., & Rubin, G. M. (2015). Optimized tools for multicolor stochastic labeling reveal
607 diverse stereotyped cell arrangements in the fly visual system. *Proceedings of the National Academy*
608 *of Sciences of the United States of America*, 112(22), E2967–76.
609 <http://doi.org/10.1073/pnas.1506763112>
- 610 Noborn, F., Gomez Toledo, A., Green, A., Nasir, W., Sihlbom, C., Nilsson, J., & Larson, G. (2016). Site-
611 specific identification of heparan and chondroitin sulfate glycosaminoglycans in hybrid
612 proteoglycans. *Scientific Reports*, 6(1), 34537. <http://doi.org/10.1038/srep34537>
- 613 Noborn, F., Gomez Toledo, A., Nasir, W., Nilsson, J., Dierker, T., Kjellén, L., & Larson, G. (2018).
614 Expanding the chondroitin glycoproteome of Caenorhabditis elegans. *Journal of Biological*
615 *Chemistry*, 293(1), 379–389. <http://doi.org/10.1074/jbc.M117.807800>
- 616 Noborn, F., Gomez Toledo, A., Sihlbom, C., Lengqvist, J., Fries, E., Kjellén, L., et al. (2015).
617 Identification of chondroitin sulfate linkage region glycopeptides reveals prohormones as a novel
618 class of proteoglycans. *Molecular & Cellular Proteomics : MCP*, 14(1), 41–49.
619 <http://doi.org/10.1074/mcp.M114.043703>
- 620 Nolo, R., Abbott, L. A., & Bellen, H. J. (2000). Senseless, a Zn finger transcription factor, is necessary
621 and sufficient for sensory organ development in Drosophila. *Cell*, 102(3), 349–362.
- 622 O'Keefe, D. D., Thor, S., & Thomas, J. B. (1998). Function and specificity of LIM domains in Drosophila
623 nervous system and wing development. *Development (Cambridge, England)*, 125(19), 3915–3923.
- 624 Olson, S. K., Bishop, J. R., Yates, J. R., Oegema, K., & Esko, J. D. (2006). Identification of novel
625 chondroitin proteoglycans in Caenorhabditis elegans: embryonic cell division depends on CPG-1 and
626 CPG-2. *The Journal of Cell Biology*, 173(6), 985–994. <http://doi.org/10.1083/jcb.200603003>
- 627 Patel, N. H., Martín-Blanco, E., Coleman, K. G., Poole, S. J., Ellis, M. C., Kornberg, T. B., & Goodman,
628 C. S. (1989). Expression of engrailed proteins in arthropods, annelids, and chordates. *Cell*, 58(5),
629 955–968.
- 630 Patel, N. H., Snow, P. M., & Goodman, C. S. (1987). Characterization and cloning of fasciclin III: a
631 glycoprotein expressed on a subset of neurons and axon pathways in Drosophila. *Cell*, 48(6), 975–
632 988.

- 633 Perrimon, N., & Bernfield, M. (2000). Specificities of heparan sulphate proteoglycans in developmental
634 processes. *Nature*, 404(6779), 725–728. <http://doi.org/10.1038/35008000>
- 635 Pfeiffer, B. D., Ngo, T.-T. B., Hibbard, K. L., Murphy, C., Jenett, A., Truman, J. W., & Rubin, G. M.
636 (2010). Refinement of tools for targeted gene expression in *Drosophila*. *Genetics*, 186(2), 735–755.
637 <http://doi.org/10.1534/genetics.110.119917>
- 638 Poulain, F. E., & Yost, H. J. (2015). Heparan sulfate proteoglycans: a sugar code for vertebrate
639 development? *Development (Cambridge, England)*, 142(20), 3456–3467.
640 <http://doi.org/10.1242/dev.098178>
- 641 Pusch, C. M., Zeitz, C., Brandau, O., Pesch, K., Achatz, H., Feil, S., et al. (2000). The complete form of
642 X-linked congenital stationary night blindness is caused by mutations in a gene encoding a leucine-
643 rich repeat protein. *Nature Genetics*, 26(3), 324–327. <http://doi.org/10.1038/81627>
- 644 Ragkousi, K., & Gibson, M. C. (2014). Cell division and the maintenance of epithelial order. *The Journal*
645 *of Cell Biology*, 207(2), 181–188. <http://doi.org/10.1083/jcb.201408044>
- 646 Ren, W., Zhang, Y., Li, M., Wu, L., Wang, G., Baeg, G.-H., et al. (2015). Windpipe controls *Drosophila*
647 intestinal homeostasis by regulating JAK/STAT pathway via promoting receptor endocytosis and
648 lysosomal degradation. *PLoS Genetics*, 11(4), e1005180.
649 <http://doi.org/10.1371/journal.pgen.1005180>
- 650 Ren, X., Yang, Z., Xu, J., Sun, J., Mao, D., Hu, Y., et al. (2014). Enhanced specificity and efficiency of
651 the CRISPR/Cas9 system with optimized sgRNA parameters in *Drosophila*. *Cell Reports*, 9(3), 1151–
652 1162. <http://doi.org/10.1016/j.celrep.2014.09.044>
- 653 Riggelman, B., Schedl, P., & Wieschaus, E. (1990). Spatial expression of the *Drosophila* segment polarity
654 gene *armadillo* is posttranscriptionally regulated by *wingless*. *Cell*, 63(3), 549–560.
- 655 Saied-Santiago, K., & Bülow, H. E. (2018). Diverse roles for glycosaminoglycans in neural patterning.
656 *Developmental Dynamics : an Official Publication of the American Association of Anatomists*,
657 247(1), 54–74. <http://doi.org/10.1002/dvdy.24555>
- 658 Schaefer, L., & Iozzo, R. V. (2008). Biological functions of the small leucine-rich proteoglycans: from
659 genetics to signal transduction. *The Journal of Biological Chemistry*, 283(31), 21305–21309.
660 <http://doi.org/10.1074/jbc.R800020200>
- 661 Schindelin, J., Arganda-Carreras, I., Frise, E., Kaynig, V., Longair, M., Pietzsch, T., et al. (2012). Fiji: an
662 open-source platform for biological-image analysis. *Nature Methods*, 9(7), 676–682.
663 <http://doi.org/10.1038/nmeth.2019>
- 664 Silver, J., & Miller, J. H. (2004). Regeneration beyond the glial scar. *Nature Reviews Neuroscience*, 5(2),
665 146–156. <http://doi.org/10.1038/nrn1326>
- 666 Smith, R. B., Machamer, J. B., Kim, N. C., Hays, T. S., & Marques, G. (2012). Relay of retrograde
667 synaptogenic signals through axonal transport of BMP receptors. *Journal of Cell Science*, 125(Pt 16),
668 3752–3764. <http://doi.org/10.1242/jcs.094292>
- 669 Strigini, M., & Cohen, S. M. (1997). A Hedgehog activity gradient contributes to AP axial patterning of
670 the *Drosophila* wing. *Development (Cambridge, England)*, 124(22), 4697–4705.
- 671 Tabata, T., & Takei, Y. (2004). Morphogens, their identification and regulation. *Development*
672 *(Cambridge, England)*, 131(4), 703–712. <http://doi.org/10.1242/dev.01043>
- 673 Takei, Y. (2004). Three *Drosophila* EXT genes shape morphogen gradients through synthesis of heparan
674 sulfate proteoglycans, 131(1), 73–82. <http://doi.org/10.1242/dev.00913>
- 675 Takemura, M., & Adachi-Yamada, T. (2011). Cell death and selective adhesion reorganize the
676 dorsoventral boundary for zigzag patterning of *Drosophila* wing margin hairs. *Developmental*
677 *Biology*, 357(2), 336–346. <http://doi.org/10.1016/j.ydbio.2011.07.007>
- 678 Takemura, M., & Nakato, H. (2015). Genetic approaches in the study of heparan sulfate functions in
679 *Drosophila*. *Methods in Molecular Biology (Clifton, N.J.)*, 1229(Chapter 38), 497–505.
680 http://doi.org/10.1007/978-1-4939-1714-3_38
- 681 Takemura, M., & Nakato, H. (2017). *Drosophila* Sulfl is required for the termination of intestinal stem
682 cell division during regeneration. *Journal of Cell Science*, 130(2), 332–343.
683 <http://doi.org/10.1242/jcs.195305>

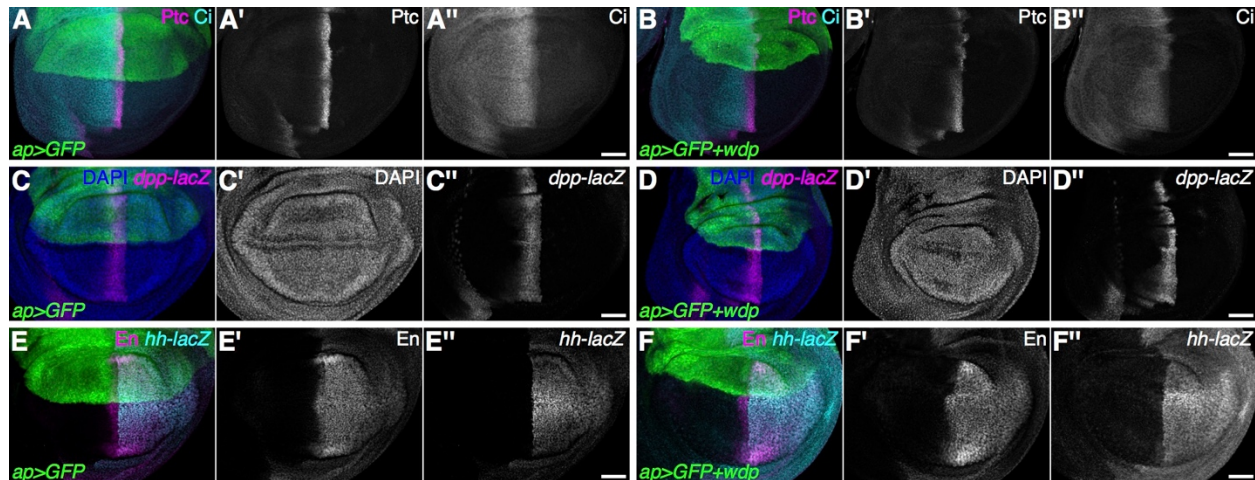
- 684 Tanimoto, H., Itoh, S., Dijke, ten, P., & Tabata, T. (2000). Hedgehog creates a gradient of DPP activity in
685 *Drosophila* wing imaginal discs. *Molecular Cell*, 5(1), 59–71.
- 686 Tavsanlı, B. C., Ostrin, E. J., Burgess, H. K., Middlebrooks, B. W., Pham, T. A., & Mardon, G. (2004).
687 Structure-function analysis of the *Drosophila* retinal determination protein Dachshund.
688 *Developmental Biology*, 272(1), 231–247. <http://doi.org/10.1016/j.ydbio.2004.05.005>
- 689 Townley, R. A., & Bülow, H. E. (2018). Deciphering functional glycosaminoglycan motifs in
690 development. *Current Opinion in Structural Biology*, 50, 144–154.
691 <http://doi.org/10.1016/j.sbi.2018.03.011>
- 692 Toyoda, H., Kinoshita-Toyoda, A., & Selleck, S. B. (2000). Structural analysis of glycosaminoglycans in
693 *Drosophila* and *Caenorhabditis elegans* and demonstration that tout-velu, a *Drosophila* gene related
694 to EXT tumor suppressors, affects heparan sulfate in vivo. *The Journal of Biological Chemistry*,
695 275(4), 2269–2275.
- 696 Van Vactor, D., Wall, D. P., & Johnson, K. G. (2006). Heparan sulfate proteoglycans and the emergence
697 of neuronal connectivity. *Current Opinion in Neurobiology*, 16(1), 40–51.
698 <http://doi.org/10.1016/j.conb.2006.01.011>
- 699 Viswanathan, S., Williams, M. E., Bloss, E. B., Stasevich, T. J., Speer, C. M., Nern, A., et al. (2015).
700 High-performance probes for light and electron microscopy. *Nature Methods*, 12(6), 568–576.
701 <http://doi.org/10.1038/nmeth.3365>
- 702 Wang, J., Al-Ouran, R., Hu, Y., Kim, S.-Y., Wan, Y.-W., Wangler, M. F., et al. (2017). MARRVEL:
703 Integration of Human and Model Organism Genetic Resources to Facilitate Functional Annotation of
704 the Human Genome. *American Journal of Human Genetics*.
705 <http://doi.org/10.1016/j.ajhg.2017.04.010>
- 706 Wang, L., Dankert, H., Perona, P., & Anderson, D. J. (2008). A common genetic target for environmental
707 and heritable influences on aggressiveness in *Drosophila*. *Proceedings of the National Academy of*
708 *Sciences of the United States of America*, 105(15), 5657–5663.
709 <http://doi.org/10.1073/pnas.0801327105>
- 710 Whalen, D. M., Malinauskas, T., Gilbert, R. J. C., & Siebold, C. (2013). Structural insights into
711 proteoglycan-shaped Hedgehog signaling. *Proceedings of the National Academy of Sciences of the*
712 *United States of America*, 110(41), 16420–16425. <http://doi.org/10.1073/pnas.1310097110>
- 713 Williams, E. H., Pappano, W. N., Saunders, A. M., Kim, M.-S., Leahy, D. J., & Beachy, P. A. (2010).
714 Dally-like core protein and its mammalian homologues mediate stimulatory and inhibitory effects on
715 Hedgehog signal response. *Proceedings of the National Academy of Sciences of the United States of*
716 *America*, 107(13), 5869–5874. <http://doi.org/10.1073/pnas.1001777107>
- 717 Xu, D., & Esko, J. D. (2014). Demystifying heparan sulfate-protein interactions. *Annual Review of*
718 *Biochemistry*, 83(1), 129–157. <http://doi.org/10.1146/annurev-biochem-060713-035314>
- 719 Xu, T., & Rubin, G. M. (1993). Analysis of genetic mosaics in developing and adult *Drosophila* tissues.
720 *Development (Cambridge, England)*, 117(4), 1223–1237.
- 721 Yan, D., Wu, Y., Yang, Y., Belenkaya, T. Y., Tang, X., & Lin, X. (2010). The cell-surface proteins
722 Dally-like and Ihog differentially regulate Hedgehog signaling strength and range during
723 development. *Development (Cambridge, England)*, 137(12), 2033–2044.
724 <http://doi.org/10.1242/dev.045740>
- 725 Zecca, M., Basler, K., & Struhl, G. (1995). Sequential organizing activities of engrailed, hedgehog and
726 decapentaplegic in the *Drosophila* wing. *Development (Cambridge, England)*, 121(8), 2265–2278.
- 727 Zecca, M., Basler, K., & Struhl, G. (1996). Direct and long-range action of a wingless morphogen
728 gradient. *Cell*, 87(5), 833–844. <http://doi.org/10.5167/uzh-996>
- 729 Zhang, F., McLellan, J. S., Ayala, A. M., Leahy, D. J., & Linhardt, R. J. (2007). Kinetic and structural
730 studies on interactions between heparin or heparan sulfate and proteins of the hedgehog signaling
731 pathway. *Biochemistry*, 46(13), 3933–3941. <http://doi.org/10.1021/bi6025424>
- 732 Zhu, A. J., Zheng, L., Suyama, K., & Scott, M. P. (2003). Altered localization of *Drosophila* Smoothed
733 protein activates Hedgehog signal transduction. *Genes & Development*, 17(10), 1240–1252.
734 <http://doi.org/10.1101/gad.1080803>

735



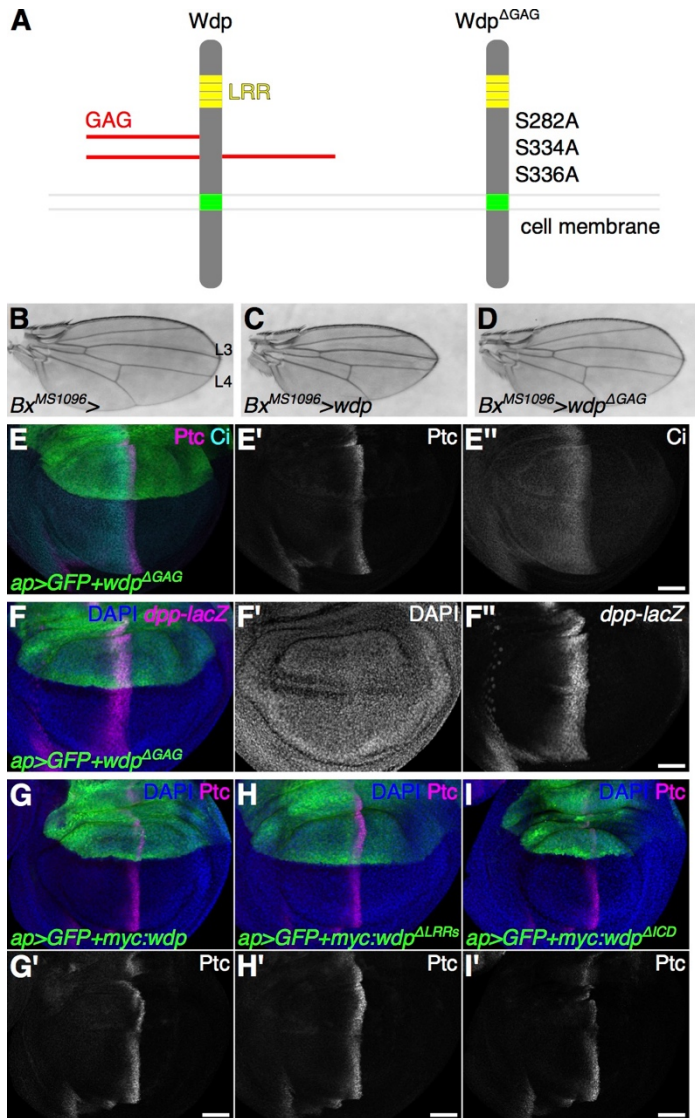
736
737

738 **Figure 1. Identification of Wdp as a novel CSPG in *Drosophila*.** (A) A scheme for identifying CSPGs
 739 in *Drosophila*. The workflow includes the enrichment of proteoglycans from fly extract, enzymatic
 740 hydrolysis and subsequent analysis and interpretation of mass spectra. (B and C) MS2 fragment mass
 741 spectra of Wdp protein (UniProt: Q9W266) showing two unique CS-glycopeptides. (B) Peptide
 742 (SDQVEGSGDLSETNMELK) identified with one hexasaccharide structure and one methionine
 743 oxidation (m/z 983.38; 3+) (C) Peptide (EEHIVKDEDEDDEGSGSGGGLLIIPDPSK) identified with two
 744 hexasaccharide structures where one of the hexasaccharides were modified with one phosphate
 745 modification (m/z 1276.76; 4+). The asterisk denotes the second isotopic peak.



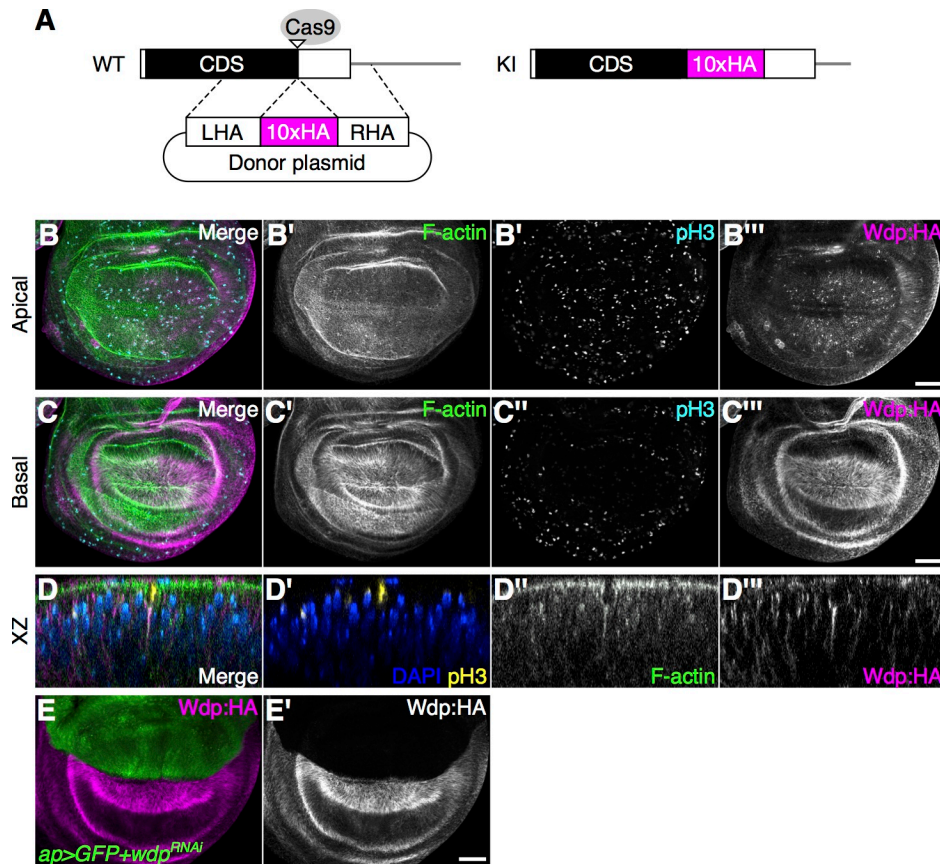
746
747

748 **Figure 2. Overexpression of *wdp* reduces the Hh-signaling-active domain.** (A–F) Control wing discs
749 (A, C, and E) and wing discs overexpressing *wdp* with *ap-GAL4* (*ap>GFP+wdp*) (B, D, and F) were
750 immunostained for the expression of Ptc, Ci (A and B), *dpp-lacZ* (C and D), En, and *hh-lacZ* (E and F).
751 The expression domains of Ptc, Ci, and *dpp-lacZ* were reduced by *wdp* overexpression in the dorsal
752 compartment compared to those in the ventral compartment. En expression induced by high-level Hh
753 signaling in the anterior compartment is diminished by *wdp* overexpression. Note that the *hh-lacZ*
754 expression is not affected by *wdp* overexpression. Nuclei were stained with DAPI (C and D). Anterior to
755 the left; dorsal to the top. Scale bars: 50 μ m.



756
757
758
759
760
761
762
763
764
765

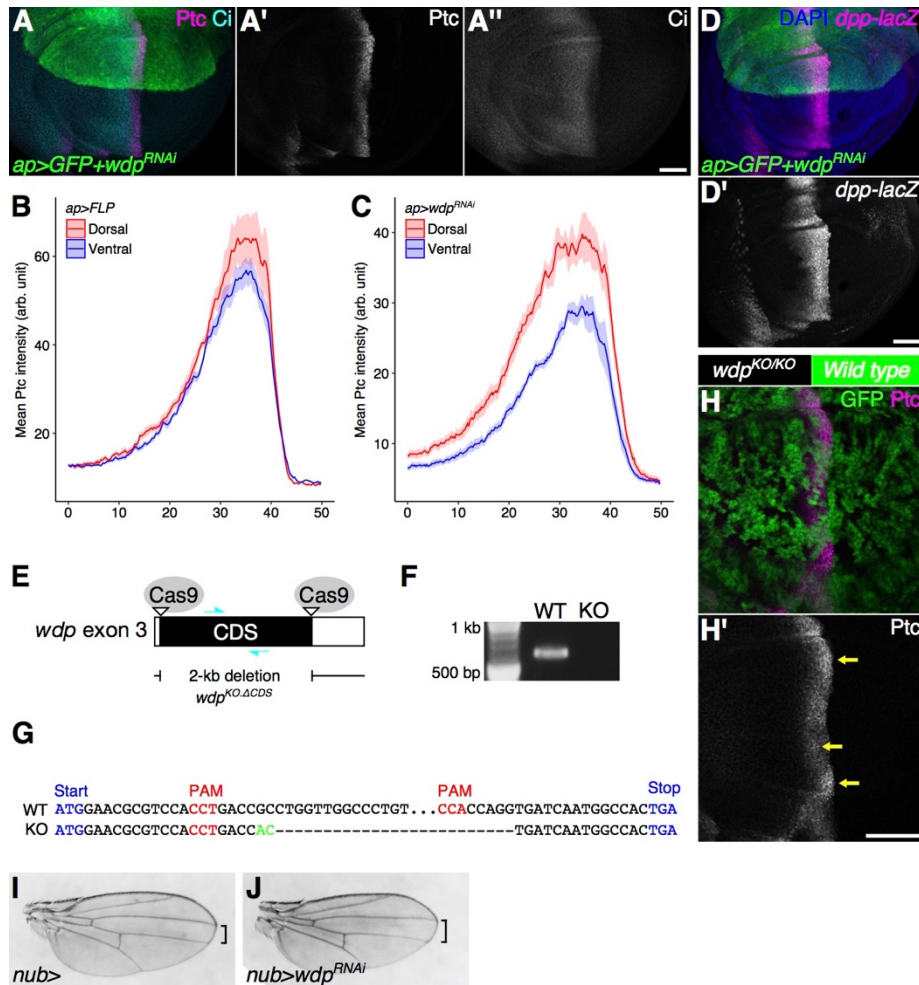
Figure 3. Wdp negatively regulates Hh signaling in a GAG-dependent manner. (A) A schematic drawing of wild-type Wdp and a mutant form of Wdp (Wdp^{ΔGAG}). (B–D) A control adult wing (B) and adult wings expressing *UAS-wdp* (C) or *UAS-wdp^{ΔGAG}* (D) with *Bx^{MS1096}-GAL4*. (E and F) Wing discs expressing *UAS-wdp^{ΔGAG}* with *ap-GAL4* were immunostained for Ptc, Ci (E) and *dpp-lacZ* (F). (G–I) Wing discs expressing *UAS-3xMyc:wdp* (G), *UAS-3xMyc:wdp^{ΔLRRs}* (H), and *UAS-3xMyc:wdp^{ΔICD}* (I) were immunostained for Ptc. Nuclei were stained with DAPI. Scale bars: 50 μm.



766
767

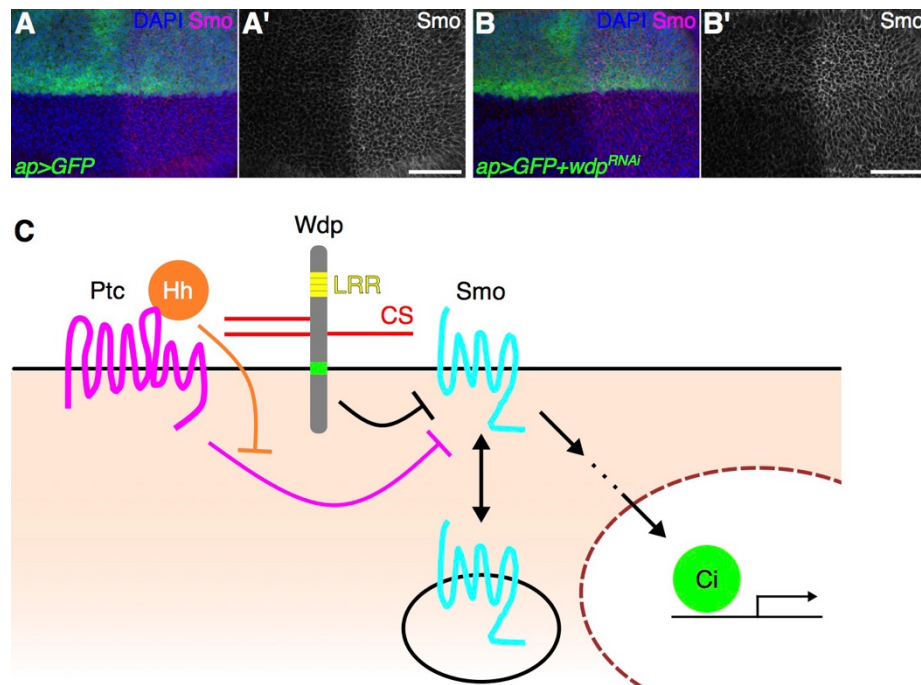
768 **Figure 4. Wdp expression in the wing disc.** (A) A schematic of CRISPR–Cas9-mediated gene editing of
769 *wdp* for generating *wdp*^{KI,HA}. Ten copies of an HA epitope tag (smGFP-HA) were inserted in frame near
770 the stop codon of the *wdp* coding sequence (CDS). Only the last exon is shown. CDS, the black box;
771 smGFP-HA, the magenta box; LHA, left homology arm; RHA, right homology arm; Cas9 target site, the
772 open triangle. (B–D) Wing discs homozygous for *wdp*^{KI,HA} were stained with Alexa Fluor 568-conjugated
773 phalloidin (F-actin), anti-phospho histone H3 antibody (pH3, mitotic nuclei), and anti-HA antibody.
774 Apical (B) and basal (C) sections of the same disc are shown. Intense staining of Wdp:HA was observed
775 on the basal side of wing disc epithelium (C–C’’’). An optical cross section shows the accumulation of
776 Wdp:HA in the basal projection of apically translocating mitotic cells (D–D’’’). (E) Wdp:HA is not
777 detectable in the dorsal compartment of a wing disc expressing *wdp*^{RNAi} (TRiP.HMC06302) with *ap*-
778 *GAL4*. Nuclei were stained with DAPI (D and E). Scale bars: 50 μm.

779



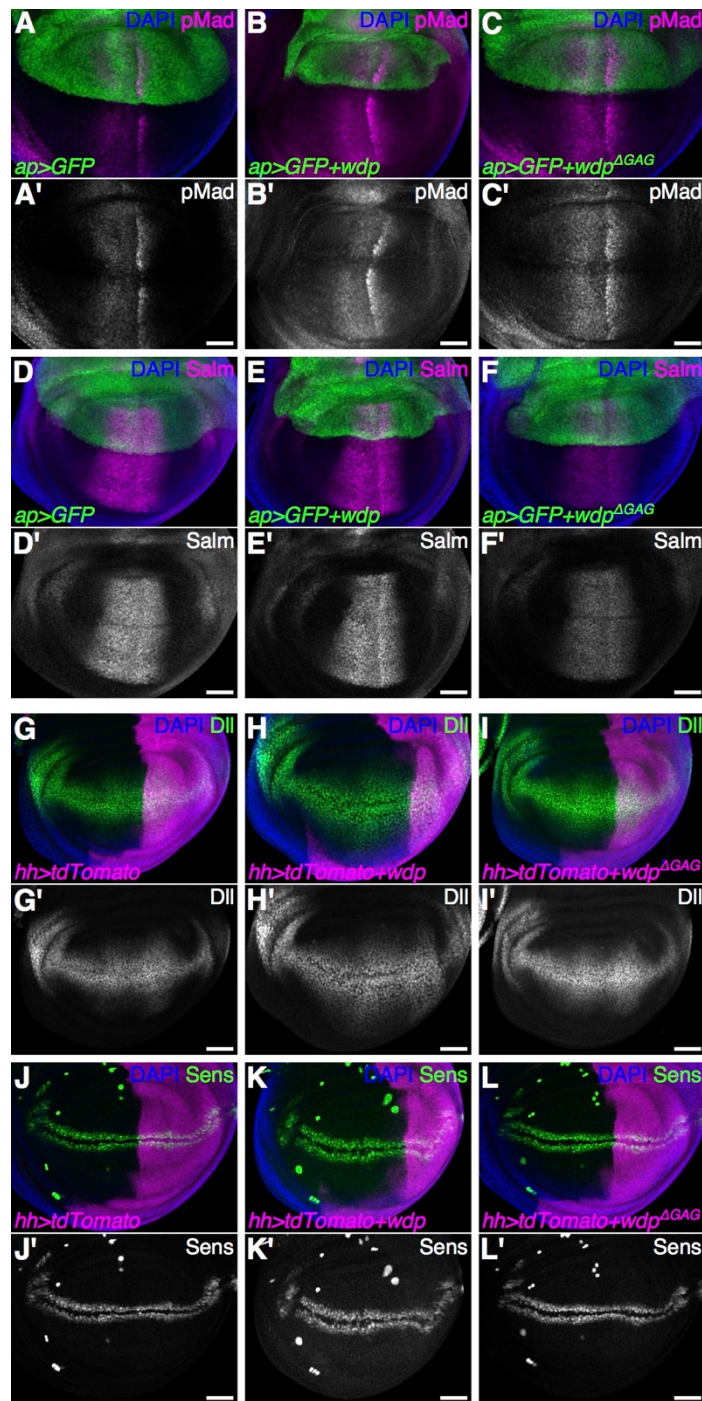
780
781
782
783
784
785
786
787
788
789
790
791
792
793
794
795
796

Figure 5. Loss of *wdp* leads to increased Hh signaling. (A) A wing disc expressing *UAS-wdp^{RNAi}* (TRiP.HMC06302) with *ap-GAL4* was immunostained for Ptc and Ci. (B and C) Signal intensity plots of the Ptc expression in the dorsal compartment (red) and ventral compartment (blue) in wing discs expressing *UAS-FLP* (B) or *UAS-wdp^{RNAi}* (C). Solid lines indicate the average intensity of Ptc staining and shaded areas show the standard error of the mean. (D) A wing disc expressing *UAS-wdp^{RNAi}* with *ap-GAL4* was immunostained for *dpp-lacZ*. Nuclei were stained with DAPI. (E) A schematic of the generation of a *wdp* loss-of-function allele (*wdp^{KO,ΔCDS}*) lacking most of the *wdp* CDS using the CRISPR–Cas9 system. (F) A PCR-based genotyping result for the wild-type (WT) and *wdp^{KO,ΔCDS}* allele (KO) using a primer set shown as cyan arrows in E. (G) Genomic sequence of the *wdp* endogenous locus targeted by CRISPR–Cas9 to delete most of the *wdp* CDS. A small insertion is shown in green. (H) Somatic mosaic clones of *wdp^{KO}* were induced in the wing pouch using *nub-GAL4 UAS-FLP*. Homozygous *wdp^{KO}* mutant cells are marked by loss of GFP. Increased Ptc expression was observed in *wdp* mutant clones (yellow arrows) (I, J) A control adult wing (I) and a wing expressing *UAS-wdp^{RNAi}* (TRiP.HM05118) (J) by *nub-GAL4*. Scale bars: 50 μm.



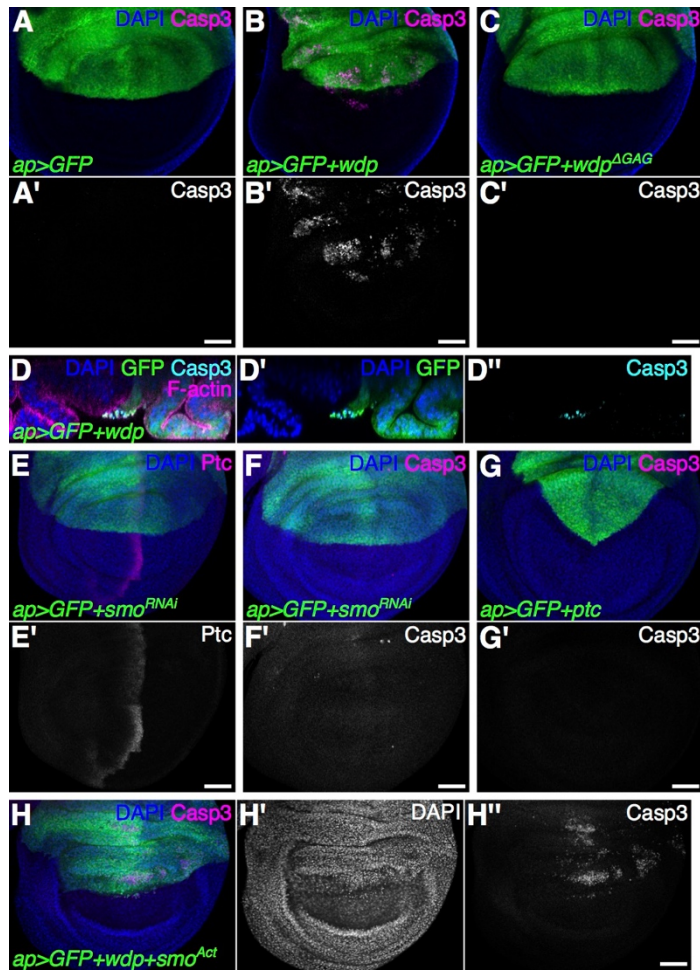
797
798
799
800
801
802
803
804

Figure 6. Wdp negatively regulates Smo cell surface accumulation. (A, B) A control wing disc and a wing disc expressing *UAS-wdp^{RNAi}* (TRiP.HMC06302) with *ap-GAL4* were immunostained for the expression of Smo. Nuclei were stained with DAPI. Scale bars: 50 μ m. (C) A model for how Wdp modulates Hh signaling. Wdp inhibits Smo cell surface accumulation thereby reducing Hh signaling activity.



805
806
807
808
809
810
811
812
813

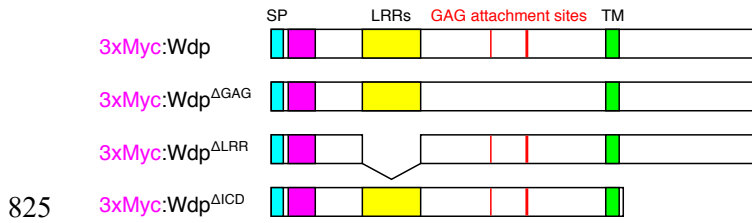
Figure S1. Effect of *wdp* overexpression on Dpp and Wg signaling. (A–F) Control wing discs (A and D) and wing discs expressing *UAS-wdp* (B and E) or *UAS-wdp*^{AGAG} (C and F) with *ap-GAL4* were immunostained for pMad (A–C) and Salm (D–F) as read-outs of Dpp signaling. (G–L) Control wing discs (G and J) and wing discs expressing *UAS-wdp* (H and K) or *UAS-wdp*^{AGAG} (I and L) with *hh-GAL4* were immunostained for Dll (G–I) and Sens (J–L) as read-outs of Wg signaling (Nolo et al., 2000; Zecca, Basler, & Struhl, 1996). Nuclei were stained with DAPI. Scale bars: 50 μ m.



814
815

816 **Figure S2. Overexpression of *wdp* in the wing disc induces apoptosis.** (A–C) A control wing disc (A)
817 and wing discs expressing *UAS-wdp* (B) or *UAS-wdp^{AGAG}* (C) with *ap-GAL4* were immunostained for
818 cleaved Caspase-3 as a marker of apoptotic cells. (D) An optical cross section of a wing disc expressing
819 *UAS-wdp* with *ap-GAL4*. Signals for cleaved Caspase-3 (cyan) and F-actin (magenta) are shown. (E) A
820 wing disc expressing *UAS-smo^{RNAi}* (TRiP.HMC03577) with *ap-GAL4* was immunostained for Ptc. (F and
821 G) Wing discs expressing *UAS-smo^{RNAi}* (F) or *UAS-ptc* (G) with *ap-GAL4* were immunostained for
822 cleaved Caspase-3. (H) A wing disc coexpressing *UAS-wdp* and *UAS-FLAG:smo^{Act}* was immunostained
823 for cleaved Caspase-3. Nuclei were stained with DAPI. Scale bars: 50 μm.

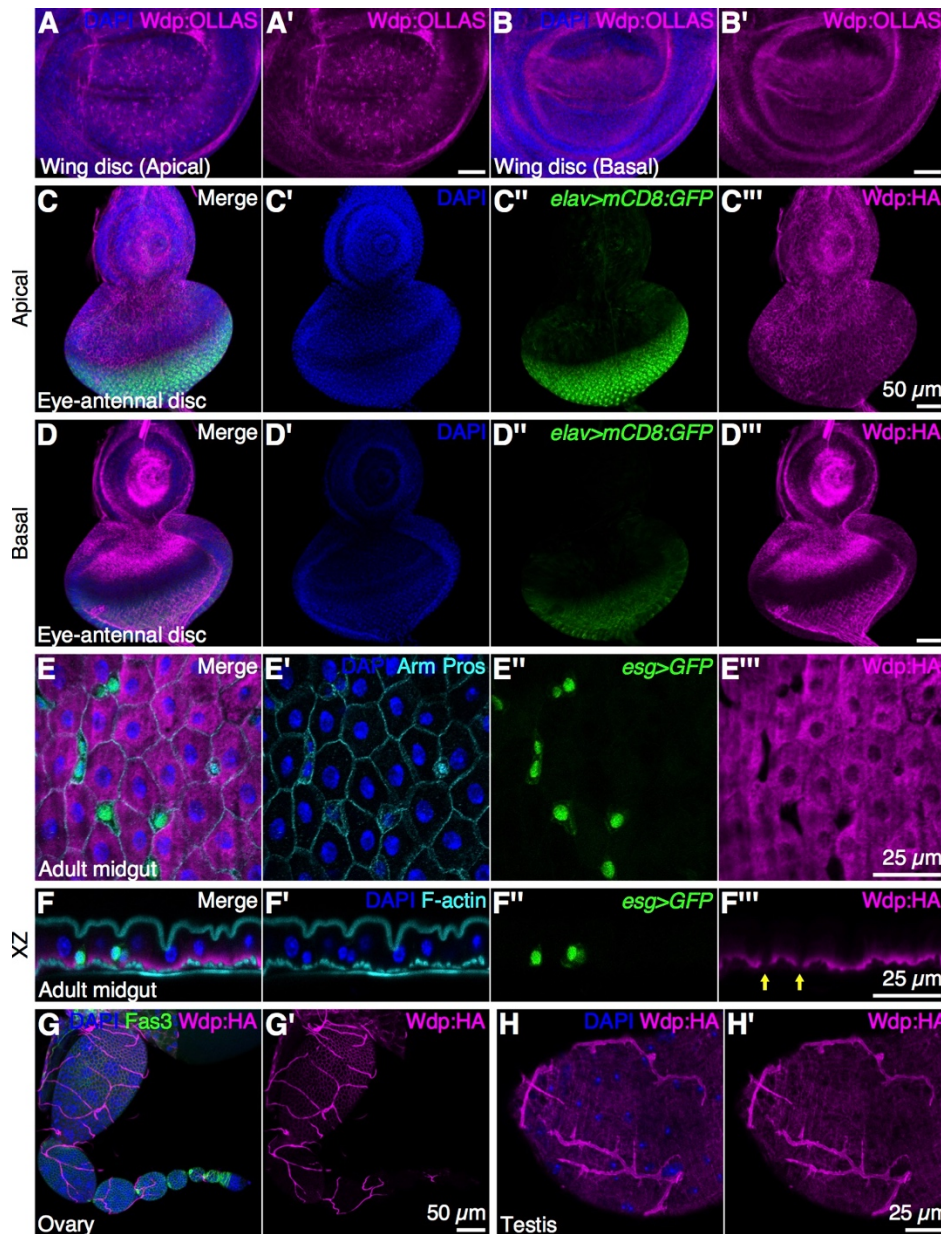
824



825
826

827 **Figure S3. A schematic of 3xMyc-tagged wild-type and mutant Wdp constructs.** The
828 magenta box denotes 3 copies of a Myc tag. The cyan box indicates the signal peptide (SP). The
829 yellow box shows the LRR motifs. The red line indicates the CS attachment sites. The green box
830 shows the transmembrane domain (TM).

831



832

833

834 **Figure S4. Expression patterns of Wdp in the eye disc, adult posterior midgut, ovary and testis.** (A,
 835 **B**) Apical (A) and basal (B) sections of a wing disc homozygous for *wdp^{KI.OLLAS}* was stained with anti-
 836 OLLAS antibody. (C–H) An eye disc, adult midgut, ovary, and testis with one or two copies of *wdp^{KI.HA}*
 837 were immunostained with anti-HA antibody (magenta). (C, D) Apical (C) and basal (D) sections of an eye
 838 disc. Neurons are marked by *elav-GAL4 UAS-mCD8:GFP* (*elav>mCD8:GFP*, green). (E) An adult
 839 midgut showing ISCs/enteroblasts (*escargot-GAL4 UAS-GFP* [*esg>GFP*]), enteroendocrine cells
 840 (nuclear Prospero [Pros]), cell membrane (Armadillo [Arm]), and Wdp:HA. (F) An optical cross section
 841 of an adult midgut showing ISCs/enteroblasts (*esg>GFP*) and F-actin (stained by phalloidin-Alexa568).
 842 (G) Wdp:HA expression is detected in the egg chambers (stage 6 and later) in the ovary. Wdp:HA is also
 843 detectable in the tracheal system. (H) Wdp:HA expression is detected in the sheath cells and the tracheal
 844 system in the testis. Nuclei were stained with DAPI. Scale bars: 50 μm (A, B, C, D, and G), 25 μm (E, F,
 845 and H).

846 **Table S1. Genotypes of *Drosophila* strains used in each figure.**
847

Figure	Panel	Genotype
2	A	<i>ap-GAL4 UAS-GFP/+</i>
2	B	<i>ap-GAL4 UAS-GFP/+; UAS-wdp/+</i>
2	C	<i>ap-GAL4 UAS-GFP dpp-lacZ/+</i>
2	D	<i>ap-GAL4 UAS-GFP dpp-lacZ/+; UAS-wdp/+</i>
2	E	<i>ap-GAL4 UAS-GFP hh-lacZ/+</i>
2	F	<i>ap-GAL4 UAS-GFP hh-lacZ/+; UAS-wdp/+</i>
3	B	<i>Bx^{MS1096}-GAL4/+</i>
3	C	<i>Bx^{MS1096}-GAL4/+; UAS-wdp/+</i>
3	D	<i>Bx^{MS1096}-GAL4/+; UAS-wdp^{AGAG}</i>
3	E	<i>ap-GAL4 UAS-GFP/+; UAS-wdp^{AGAG}/+</i>
3	F	<i>ap-GAL4 UAS-GFP dpp-lacZ/+; UAS-wdp^{AGAG}/+</i>
3	G	<i>ap-GAL4 UAS-GFP/+; UAS-3xMyc:wdp/+</i>
3	H	<i>ap-GAL4 UAS-GFP/+; UAS-3xMyc:wdp^{ALRRs}/+</i>
3	I	<i>ap-GAL4 UAS-GFP/+; UAS-3xMyc:wdp^{ΔICD}/+</i>
4	B, C, D	<i>wdp^{KLHA}/wdp^{KLHA}</i>
4	E	<i>ap-GAL4 UAS-GFP wdp^{KLHA}/UAS-wdp^{RNAi.HMC06302}</i>
5	A, C	<i>ap-GAL4 UAS-GFP/UAS-wdp^{RNAi.HMC06302}</i>
5	B	<i>ap-GAL4 UAS-GFP/UAS-wdp^{RNAi.HMC06302}</i>
5	D	<i>ap-GAL4 UAS-GFP dpp-lacZ/UAS-wdp^{RNAi.HMC06302}</i>
5	H	<i>nub-GAL4, FRT42D wdp^{KO.ΔCDS}/FRT42D 2xubi-GFP; UAS-FLP/+</i>
5	I	<i>nub-GAL4/+</i>
5	J	<i>nub-GAL4/+; UAS-wdp^{RNAi.HMS05118}/+</i>
6	A	<i>ap-GAL4 UAS-GFP/+</i>
6	B	<i>ap-GAL4 UAS-GFP/UAS-wdp^{RNAi.HMC06302}</i>
S1	A, D	<i>ap-GAL4 UAS-GFP/+</i>
S1	B, E	<i>ap-GAL4 UAS-GFP/+; UAS-wdp/+</i>
S1	C, F	<i>ap-GAL4 UAS-GFP/+; UAS-wdp^{AGAG}/+</i>
S1	G, J	<i>hh-GAL4 UAS-tdTomato/+</i>
S1	H, K	<i>hh-GAL4 UAS-tdTomato/UAS-wdp</i>
S1	I, L	<i>hh-GAL4 UAS-tdTomato/UAS-wdp^{AGAG}</i>
S2	A, D	<i>ap-GAL4 UAS-GFP/+</i>
S2	B	<i>ap-GAL4 UAS-GFP/+; UAS-wdp/+</i>
S2	C	<i>ap-GAL4 UAS-GFP/+; UAS-wdp^{AGAG}/+</i>
S2	E, F	<i>ap-GAL4 UAS-GFP/UAS-smo^{RNAi.HMC03577}</i>
S2	G	<i>ap-GAL4 UAS-GFP/UAS-ptc</i>
S2	H	<i>ap-GAL4 UAS-GFP/UAS-FLAG:smo^{Act}; UAS-wdp/+</i>
S4	A, B	<i>wdp^{KL.OLLAS}/wdp^{KL.OLLAS}</i>
S4	C, D	<i>elav-GAL4 UAS-mCD8:GFP/+; wdp^{KLHA}/+</i>
S4	E, F	<i>esg-GAL4 UAS-GFP/+; wdp^{KLHA}/+</i>
S4	G, H	<i>wdp^{KLHA}/wdp^{KLHA}</i>

848
849
850